Electronic Supplementary Information (ESI) for Green Chemistry:

Catalyst-free, scalable heterocyclic flow photocyclopropanation

Viktor Klöpfer[a], Robert Eckl[a], Johannes Floß[a], Phillippe Roth[b], Oliver Reiser*[a], Joshua P. Barham*[a]

[a.] V. Klöpfer, R. Eckl, J. Floß, Prof. Dr. O. Reiser, Dr. J. P. Barham
Universität Regensburg, Fakültat für Chemie und Pharmazie, Regensburg, 93040 (Germany)
E-mail: Oliver.Reiser@chemie.uni-regensburg.de ; Joshua-Philip.Barham@chemie.uni-regensburg.de
[b.] Dr. P. Roth, Corning SAS Reactor Technologies, 7 bis, Avenue de Valvins, CS 70156 Samois-sur-Seine, F - 77 210 AVON Cedex (France)

Table of Contents

1 General Information

Reagents, solvents and working methods

Starting materials and reagents were purchased from Sigma Aldrich, Fluka, VWR, Acros or Alfa Aesar and were used without further purification. Solvents for reaction mixtures were used as purchased or were dried according to common procedures.

Nuclear magnetic resonance spectroscopy (NMR)

NMR spectra were recorded using a Bruker Avance 400 (^{1}H: 400 MHz, ^{13}C: 101 MHz, T = 298 K) instrument. All chemical shifts are reported in δ [ppm] (multiplicity, coupling constant J, number of protons, assignment of proton) relative to the solvent residual peak as the internal standard. All spectra were recorded in CDCl$_3$ (δ = 7.26 ppm in ^{1}H NMR, δ = 77.16 ppm in ^{13}C NMR). The spectra were analyzed by first order and coupling constants J are given in Hertz [Hz] and are uncorrected. Abbreviations used for ^{1}H NMR signal multiplicity: s = singlet, br. s = broad singlet, d = doublet, dd = doublet of a doublet, ddd = doublet of a doublet of a doublet, ddt = doublet of a doublet of a triplet, t = triplet, q = quartet, m = multiplet, b = broad.

Chromatography

Thin-layer chromatography (TLC) was performed with TLC precoated aluminum sheets (Machery-Nagel TLC sheets ALUGRAM Xtra SIL G/UV$_{254}$, thickness 0.2 mm). Visualization was accomplished by a dual short (λ = 254 nm) / long (λ = 366 nm) wavelength UV lamp. Where necessary, staining was done with a vanillin (6.0 g vanillin in 100 mL ethanol) or potassium permanganate (1.0 g KMnO$_4$ and 2.0 g Na$_2$CO$_3$ in 100 mL water) solution. Column chromatography was performed using silica gel (Merck Geduran Si 60, 0.063-0.200 nm particle size) and/or flash silica gel 60 (Merck Geduran Si 60, 0.040-0.063 nm particle size) as the stationary phase in glass columns with either G2 or G3 frits.

UV/Vis spectroscopy

UV/Vis spectroscopy was carried out on an Analytik jena Specord® 200Plus. All compounds were measured at 10 µM in dimethylcarbonate in a 10 x 10 mm quartz cuvette; the solvent used for their preparative flow reactions. Measurement range was from 190 nm to 1100 nm.

Mass spectrometry

Mass spectrometry was performed in the Central Analytical Department of the University of Regensburg on an Agilent Technologies 6540 UHD Accurate-Mass Q-TOF LC/MS. Masses observed are accurate to within ±5 ppm. The Ionization method is noted at the analytical data of each compound (ESI = electrospray ionization, EI = electron ionization)

IR spectroscopy

ATR-IR spectroscopy was carried out on a Biorad Excalibur FTS 3000 MX, equipped with a Specac Golden Gate Diamond Single Reflection ATR-System or on an Agilent Technologies Cary 630 FTIR. Solid and liquid compounds were measured neat as a thin film.

X-Ray Crystallography

X-ray crystallographic analysis was performed by the Central Analytic Department of the University of Regensburg using an Agilent Technologies SuperNova, Single clear colourless block-shaped crystals of **3la** were used as supplied. A suitable crystal with dimensions $0.14 \times 0.13 \times 0.11$ mm^3 was selected and mounted on a MITIGEN holder oil on a XtaLAB Synergy R, DW system, HyPix-Arc 150 diffractometer. The crystal was kept at a steady $T =$ 123.00(10) K during data collection. The structure was solved with the ShelXT 2018/2 (Sheldrick, 2018) solution program using dual methods and by using Olex2 1.3-alpha (Dolomanov et al., 2009) as the graphical interface. The model was refined with ShelXL 2018/3 (Sheldrick, 2015) using full matrix least squares minimisation on F^2.

Setup of the Photochemical Flow Reactor

All flow reactions were performed in a *Corning® Advanced-Flow^{TM} Lab Photo Reactor* (Figure S1a). The reactor comprised of one fluidic module type G1 LF (glass) for low flow rates, two LED panels composed of 6 x 20 LED each (20 LEDs of each wavelength on each panel, irradiation from both sides, radient power of each LED at 100%: 1360 mW (700 mA), therefore 27.2 W input power for each panel), a dual piston pump with a metal-free Teflon pump head, an adjustable back pressure regulator (BPR) and two thermostat units (for controlling temperature of LEDs and for controlling the user-specified temperature of the fluidic module). Settable wavelengths of the LEDs were 340, 375, 395, 420, 450 and 530 nm; 450 nm was used throughout this study as guided by the UV/Vis spectra of diazoesters. The fluidic module was designed for the mixture of one or two flow paths and had a total reactor volume of 2.7 mL (Figure S1b). In order to mitigate background photodegradation or evaporation of arene substrate, pre-prepared reaction mixture feedstocks were maintained in an ice bath and in the dark before pumping into the reactor system via the dual piston pump. Depending on the reaction mixture concentration, the adjustable back pressure regulator was set between 10-18 bars (0.1 M = 10 bars, 0.3 M = 18 bars) to keep nitrogen – which evolved during photolysis of the diazoesters – in solution and thus to ensure a constant flow rate. The pressure in the reactor was monitored by a pressure sensor integrated into the pump module. For safety and to maintain integrity of the fluidic module, the maximal allowed pressure was set to 18 bar on the pump sensor such that exceeding 18 bar pressure ceased the flow. A schematic is depicted in Figure S2.

a)   b)
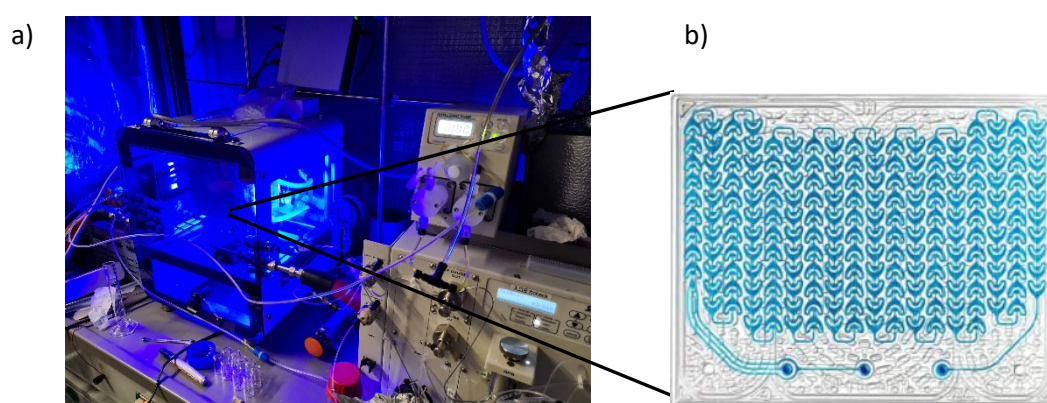
Figure S1. a) Photo of the reactor setup with the corning reactor on the left-hand side and the pump system on the right-hand side. b) fluidic microchip with a volume of 2.7 mL. Picture used with permission by © 2017 Corning Incorporated.

450 nm

18 bar

BPR

0.4 - 1.0
mL min^{-1}

450 nm

R_T **= 2.7 - 6.75 min**

N$_2$

feedstock
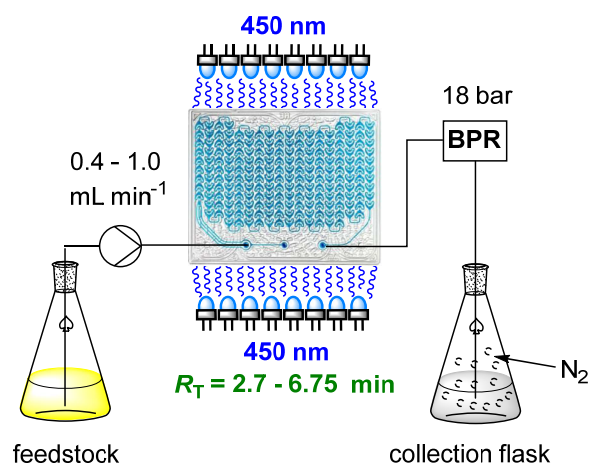
collection flask

Figure S2. Schematic of the flow reactor set-up including the Corning reactor, reaction mixture feedstock, pump, fluidic module (2.7 mL), BPR and collection flask. Picture used with permission by © 2017 Corning Incorporated.

## 2 Software-supported Optimization by Design of Experiment (DoE)

A design space for optimization was chosen by the reliable operational limits of the factors of interest as well as prior knowledge of the system:

Flow rate "Q" = 0.4 (lowest precise flow rate of the pump module under the conditions of back-pressure) → 1.0 mL/min {poor conversion due to too short residence time};

Light intensity "I_L" = 0 → 100% (as defined by the reactor system);

equivalents of **1a** from 1 → 9 (aiming for the compromise of lowest possible equivalents of **1a** while prioritizing highest possible selectivity and yield).

Experiments at the extremes of the design space were investigated, along with replicate center points to model a 3-dimensional response surface and predict the optimal conditions or to predict the next iteration of design space based by statistical software analysis. The software *Design Expert Version 12* by *StatEase®* was used to interpret the results and to build a statistical model to fit the experimental data (by ANOVA). During the DoE, a "two-level full factorial" (TFF) design and subsequent face-centered central composite (FCC) design was carried out. For TFF, M^n experiments were required, where M is the number of levels and n is the number of factors. In this case, 8 (= 2^3) experiments were performed without counting center points or replicates (Figure 3a). FCC design contains an embedded factorial design with center points that are amplified with a group of star points at the center of each face of the factorial space, for curvature modelling (Figure 3b). TFF design results are in Table S1.
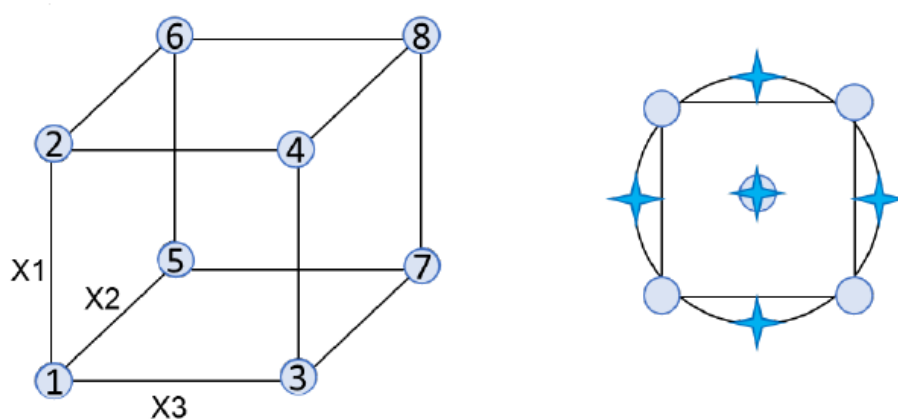

Figure S3 a) Two-level full factorial (TFF) design with three factors and b) 2-dimensional view of the 3-dimensional (cube) face-centered central composite (FCC) design for DoE study.

Table S1. Results of the Two-level Full Factorial (TFF) Design: Photoinduced Cyclopropanation of Furan (**1a**)

Std	Run	A: Substrate **1a** [equiv]	B: Q [mL/min]	C: I_L [%]	C[a] of **2a** [%]	Y[a] of **3a** [%]	S[a] to **3a** [%]	P[a] of **3a** [mg/h]
6	1	9	0.4	100	85	79	92	408
11	2	5	0.7	75	55	53	96	483
4	3	9	1.0	50	34	30	90	396
3	4	1	1.0	50	33	20	62	265
9	5	5	0.7	75	57	53	92	478
1	6	1	0.4	50	68	36	52	185
2	7	9	0.4	50	63	59	94	308
10	8	5	0.7	75	57	52	92	475
7	9	1	1.0	100	52	27	53	352
8	10	9	1.0	100	51	47	91	608
12	11	5	0.7	75	62	61	98	557
5	12	1	0.4	100	87	51	58	263
13	13	5	0.7	75	61	58	96	527

[a]determined by quantitative NMR analysis by addition of 1,3,5-trimethoxybenzene as an internal standard before running the experiments, estimated error ±5%. P = productivity, Y = yield, C = conversion, S = selectivity.

For the analysis, the data were fitted into the model which gave the best statistical fit according to ANOVA (analysis of variance). For conversion and selectivity, a linear model was most suitable. In the case of yield and productivity, a decadic logarithmic model fitted most. From the TFF design analysis, half normal plots were obtained, which graphically identify whether or not factors and factor interactions had a significant effect on the given response and compare the degree of their influence qualitatively (Figure S4). The green triangles on each graph intersected by the red line represented the experimental error derived from replicates of the center data points. Factors close to the intersecting red line carried an insignificant effect, while the relative distance of the other factors from that line indicated their degree of influence. It could be seen that none of the four responses was influenced by an interaction. In the case of conversion, the factor Q had a negative (longer R_T leading to higher conversion) while the factor I_L had a positive influence on the response (Figure S4a). The yield was controlled by all three factors, with only Q having a negative effect (Figure S4b). Selectivity, defined as the proportion of productive conversion (%Selectivity = %yield/%conversion × 100) was not affected by either Q or I_L, but the ratio between substrates was crucial for this response (Figure S4c). Productivity was positively influenced by all three factors (Figure S4d). While all the influences of the singular factors on each response were as expected, it could not be assumed that no interactions between the factors affected the outcome of the runs. Thus, the results indicated a simple factor-response correlation.
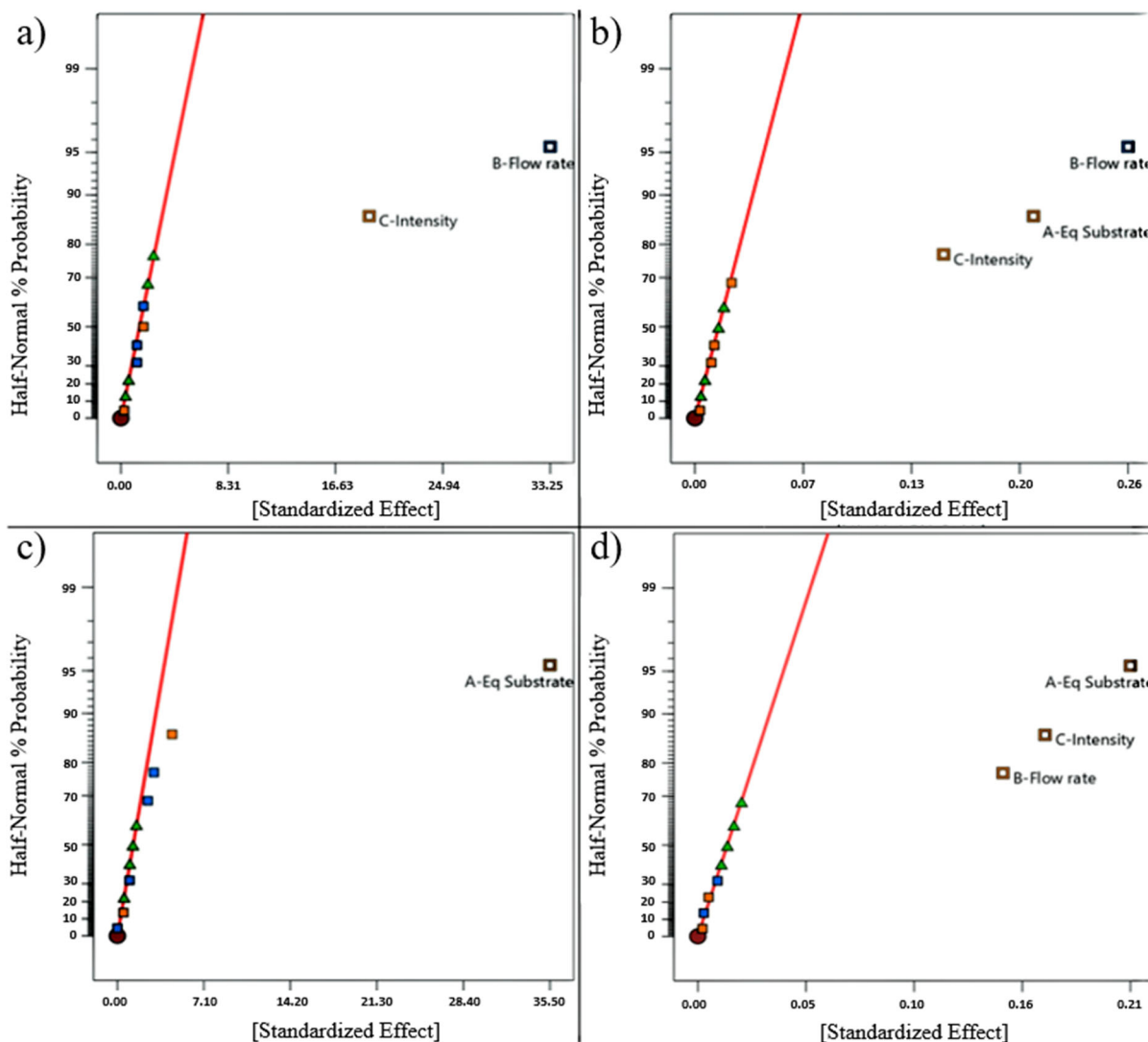
Figure S4. Evaluation of significant effects of the factors on each response by Shapiro test. Statistically based calculations with $\alpha = 0.05$ showed the qualitative effect. Orange squares (■) symbolizing positive, blue squares (■) symbolizing a negative impact on the responses, the experimental error was symbolized by the green triangles (▲). a) conversion of **2a**, b) yield of **3a**, c) selectivity towards **3a** and d) productivity of **3a**. "Eq substrate" (**A**) stands for the equivalents of substrate **1a** in respect to 1 equiv of **2a**. Flow rate (**B** = Q) was given in mL/min. "Intensity" stands for relative light intensity (**C** = I_L).

While the TFF design could sufficiently compare the effects of different experimental factors, it is unable to model data curvature and was therefore inappropriate for accurate result predictions. This can be seen in the higher standard error of design moving in any direction away from the center points (Figure S5). Therefore, a face-centered central composite (FCC) design was employed to determine the optimized reaction conditions. The TFF design was augmented with an additional six experiments (a "star design"). Usually, this star design employs data points outside of the TFF cube to minimize the standard error of design further,

however longer R_T than 6.7 mL/min and more than 100% of I_L could not practically be achieved due to instability of flow rates at lower than 0.4 mL/min and other instrumental limits (negative intensity, flow rate and equivalents are impossible). Therefore, the star points of the FCC design were positioned on the faces of the cube (Figure S3b). Its results are given in Table S2.
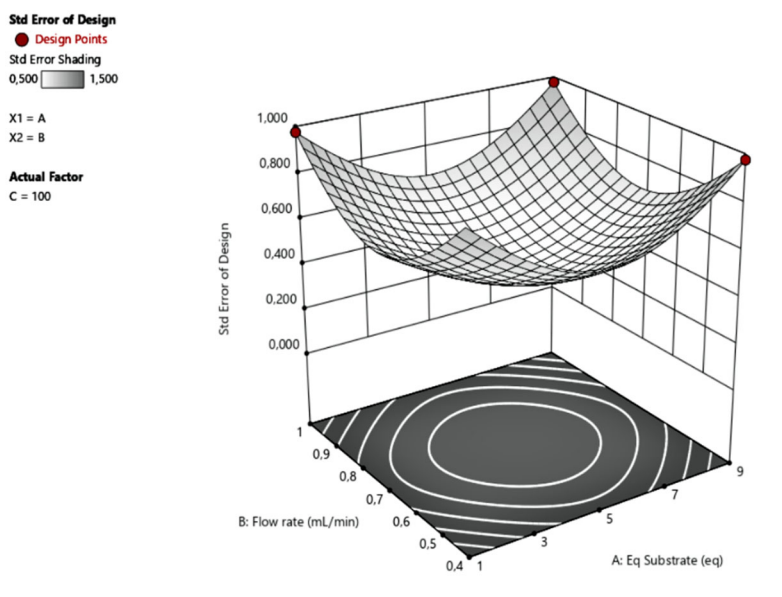
Figure S5. Statistical standard error for two-level full factorial (TFF) design.

Table S2. Results of the Face-Centered Central Composite Design: Cyclopropanation of Furan (**1a**)

Std	Run	A: Substrate 1a [equiv]	B: Q [mL/min]	C: I_L [%]	C[a] of 2a [%]	Y[a] of 3a [%]	S[a] to 3a [%]	P[a] of 3a [mg/h]
8	1	9	1.0	100	51	47	91	608
14	2	5	0.7	100	68	70	104	639
15	3	5	0.7	75	55	53	96	483
6	4	9	0.4	100	85	79	92	408
5	5	1	0.4	100	87	51	58	263
2	6	9	0.4	50	63	59	94	308
10	7	9	0.7	75	60	56	94	509
19	8	5	0.7	75	57	52	92	475
4	9	9	1.0	50	34	30	90	396
17	10	5	0.7	75	57	53	92	478
18	11	5	0.7	75	62	61	98	557
11	12	5	0.4	75	75	68	92	355
12	13	5	1.0	75	40	37	93	481
9	14	1	0.7	75	59	37	62	334
3	15	1	1.0	50	33	20	62	265
7	16	1	1.0	100	52	27	53	352
13	17	5	0.7	50	40	38	96	349
16	18	5	0.7	75	61	58	96	527
1	19	1	0.4	50	68	36	52	185

[a]determined by quantitative NMR analysis by addition of 1,3,5-trimethoxybenzene as an internal standard before running the experiments, estimated error $\pm$5%. P = productivity, Y = yield, C = conversion, S = selectivity

The analysis of the FCC design led to the modeling of the curvatures for each response (Figure S6).
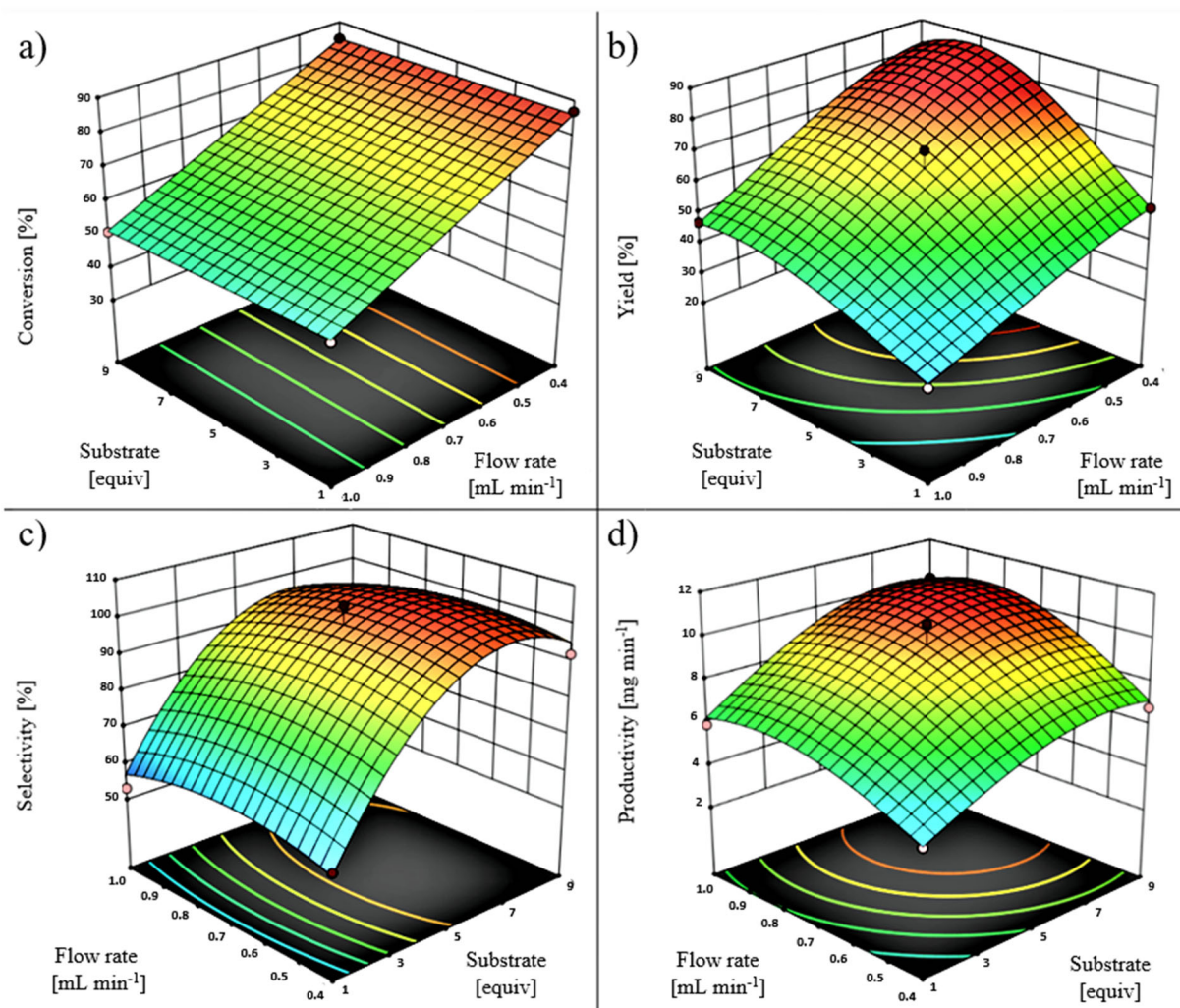
Figure S6. Statistically-calculated 3-dimensional response surface for a) conversion, b) yield, c) selectivity and d) productivity. All shown curves are for I_L = 100%. Low and high values of the responses are symbolized by cold and warm areas on the curves.

Conversion and selectivity followed a linear model, while for yield an inverse square root model and productivity a decadic logarithm model were most suitable. For all responses, the optimum lay in the investigated design space for the used reactor system. Both, the graph of productivity and the curve of selectivity showed their maximum in the studied range. In the case of yield and conversion, the curves indicated that with a longer R_T the results of both responses could be further improved. However, preliminary experiments showed that slower flow rates led to a larger error in the R_T and the outcome of the experiments became subject to a larger variation. In addition, it was evident from the response surfaces that an excess of furan was essential to maintain high yield, selectivity, and productivity. Unreacted furan (**1a**) was recovered easily by distillation.

The statistical models were confirmed by further validation experiments setting certain conditions and comparing the results predicted by the model and the experimental results. In this sense, the results of three new conditions were examined, which had not yet been performed during the DoE or OFAT study. While two experiments aimed only to validate the response surface, a third experiment aimed to both validate the response surface and to confirm the results of the predicted optimal conditions. To determine our 'optimal' conditions, the 'desirability' algorithm of the software was employed - selectivity was assigned the highest desirability, yield and productivity the second highest, and conversion the lowest desirability. A highly productive and effective process would be economically more attractive than a process at quantitative conversion but with lower efficiency, especially in this reaction, in which the unconsumed substrates are easily recovered. The results of the confirmation runs are summarized in Table S3. The means of the predicted results are given in parentheses. The comparison of the experimental and predicted values is based on statistical calculations. The software specified a range around the predicted value. If the value of the actual result lied within this calculated range, then it was valid with a confidence interval of 95% that the difference between the determined and the predicted result was insignificant. The error type I was therefore 5% (in summary for both sides of the Gaussian curve), i.e. the probability that an actual value, in reality, differed significantly from the predicted value, but this was not identified, was 5%. All experimental values of the conversion (entries 1-3), the measured values of the yields, as well as the productivity of entries 1 and 3 were just outside the calculated space, but the analytics by quantitative NMR was subject to an estimated error of $\pm$5%. Given the likely overlap of the analytical and DoE response surface errors, the agreement is overall reasonable. Since the predicted values of the other responses were confirmed, the response surface model was experimentally validated.

Table S3. Confirmation of the obtained model by performing of three runs three times. Conditions of entry 1: **2a** 1 equiv : 4 equiv **1a**, R_T = 3.4 min, I_L = 80%; entry 2: **2a** 1 equiv : 7 equiv **1a**, R_L = 4.7 min, I_L = 100%; entry 3: **2a** 1 equiv : 8 equiv **1a**, R_T = 6 min, I_L = 60%. The "Data Mean" has to lie within the space between "95% low" and "95% high". This space is calculated for an error type I of 5% (both sides of the Gaussian curve). The concentration was 0.1 M with respect to **2a** for all experiments.

Entry	Response	Predicted Mean	Std. Error	n	95% low	Data Mean[a]	95% high
1	Productivity [mg/h]	502.8756	39.18942	3	471.0546	**594.3594**	536.8458
	Yield	46.9422%	3.26076%	3	42.1041%	**55.2936%**	52.2631%
	Conversion	54.9132%	2.93467%	3	50.921%	**61.6667%**	58.9053%
	Selectivity	90.0486%	3.75104%	3	84.2236%	89.6667%	95.8736%
2	Productivity [mg/h]	558.762	43.5447	3	495.7536	605.9196	629.778
	Yield	79.4315%	7.16394%	3	66.3135%	81.6731%	95.5709%
	Conversion	75.7432%	2.93467%	3	71.1905%	**83.6667%**	80.2958%
	Selectivity	102.927%	3.75104%	3	95.3594%	97.6667%	110.494%
3	Productivity [mg/h]	361.2288	28.1508	3	325.5942	**463.8366**	400.764
	Yield	63.4598%	5.12046%	3	54.6024%	**74.2909%**	73.8756%
	Conversion	65.5132%	2.93467%	3	60.8841%	**76.0000%**	70.1422%
	Selectivity	95.2676%	3.75104%	3	88.2628%	96.3333%	102.272%

[a]determined by quantitative NMR analysis by addition of 1,3,5-trimethoxybenzene as an internal standard before running the experiments, estimated error $\pm$5%.

Entry 2 represents the optimal conditions in the specified sense and the best results. It is noteworthy that, due to the position of the star designs on the faces of the cube, the errors on the prediction become larger at the edges of the design space (Figure S7).
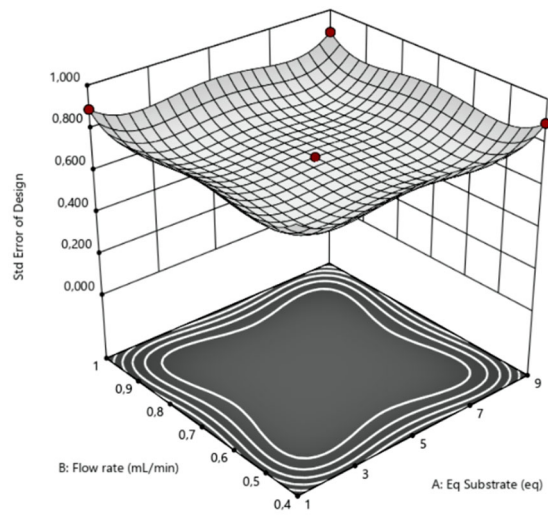
Figure S7. Statistical standard error for face-centered central (FCC) composite model.

3 UV/Vis Spectra of the Diazoacetates
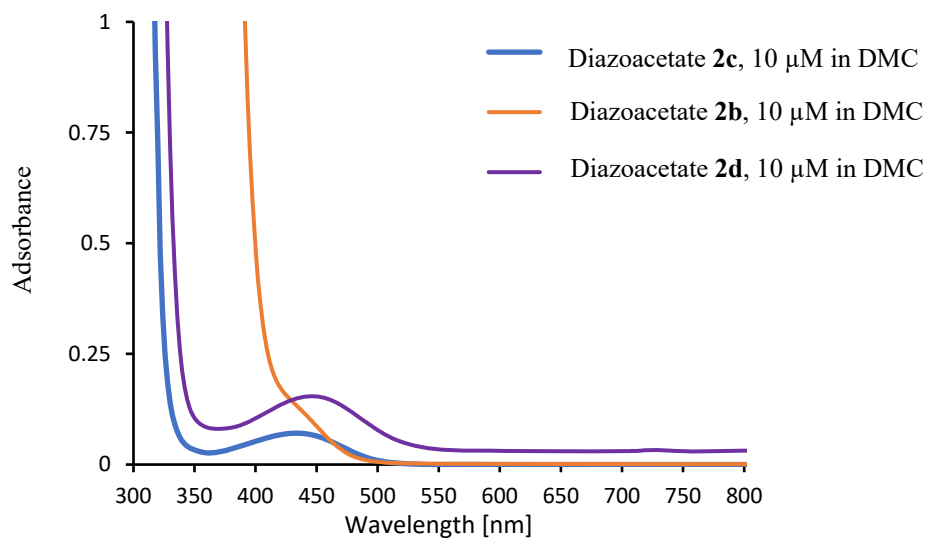
Figure S8. UV/Vis spectra of the synthesized aryl diazoacetates **2b-d**. The spectra of **2a** (50 μM) was reported by Davies *et al*.[1]

4 Synthesis and analytical Data

4.1 Starting Material Synthesis

Heterocycles **1a**, **1b**, **1c**, **1d, 1e** and **1l** were purchased and used without further purification. Cyclopentadiene (**1f**) was freshly distilled from its dimer. Heterocycles **1g-k** were readily available and synthesized according to the common procedures. Their analytical data are consistent with the literature.[2, 3, 4]

4-methylbenzenesulfonyl azide (TsN₃)

*CAUTION: Sodium azide (**NaN₃**) can decompose explosively above its melting point. It forms explosive azides with metals such as Cu, Pb, Hg, Ag, Au, and reacts with acids to form hydrazoic acid (HN₃) which is a toxic, spontaneously explosive gas. Chlorinated solvents should be avoided. All work with NaN₃ should be conducted behind a shield and in a fume hood. Excess NaN₃ is destroyed in a fume hood by oxidation with cerium(IV) ammonium nitrate. → K. Turnbull, B. Narsaiah, J. S. Yadav, T. Yakaiah, B. P. V. Lingaiah, Sodium Azide, Encyclopedia of Reagents for Organic Synthesis, 2008, Wiley.*

TsN₃
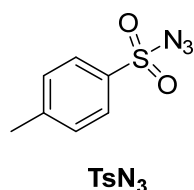
p-Toluenesulfonylchloride (36.2 g, 190 mmol, 1.0 equiv) was dissolved in acetone (200 mL) and water (200 mL). Then **NaN₃** (12.9 g, 199 mmol, 1.1 equiv) was added in portions at 0 °C and the mixture was stirred for 2.5 h at 0 °C. The reaction mixture was concentrated under reduced pressure to half of its volume. The aqueous phase was extracted with Et₂O (3 × 70 mL) and the combined organic phases were dried over MgSO₄. Evaporation of the solvent yielded **TsN₃** (37.3 g, 181 mmol, > 99%) as a colorless oil.

¹H NMR (400 MHz, CDCl₃): δ = 7.84 (d, J = 8.4 Hz, 2H), 7.41 (d, J = 8.0 Hz, 2H), 2.48 (s, 3H).

The analytical data were consistent with the literature.[5]

*CAUTION: Tosyl azide (**TsN₃**), while one of the safer azides and whose utility in the preparation of diazo compounds is noted, thermally decomposes above 120 °C and should be handled at room temperature or below.* → (a) G. G. Hazen, L. M. Weinstock, R. Connell, F. W. Bollinger, *Synth. Comm.* 1981, **11**, 947-956; (b) P. Cardillo, L. Gigante, A. Lunghi, A. Fraleoni-Morgera, P. Zanirato, *New. J. Chem.* 2008, **32**, 47-53; (c) Bretherick's Handbook of Reactive Chemical Hazards, P.G. UrbenElsevier, Amsterdam, 2007.

methyl 2-diazo-2-phenylacetate (2a)

2a
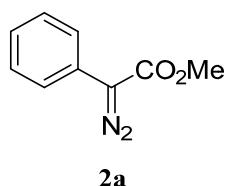
*CAUTION: All aryl diazo esters in the following section were treated as per the title compound. The title compound (**2a**) is stable to storage at room temperature or below. No difficulty was experiences after several years of studying this compound. However, caution is exercised in handling this compound due to its explosive potential; especially heating should be avoided. It is recommended that all procedures using this compound be conducted behind a blast shield* → H. M. L. Davies, W.-h. Hu, D. Xing, Methyl Phenyldiazoacetate, *Encyclopedia of Reagents for Organic Synthesis*, 2015, Wiley.

DBU (29.81 g, 195.8 mmol, 1.5 equiv) was added dropwise to a solution of methyl 2-phenylacetate (16.60 g, 160.6 mmol, 1.0 equiv) and TsN₃ **4** (38.62 g, 195.8 mmol, 1.5 equiv) in dry MeCN (150 mL) at room temperature under nitrogen atmosphere. After stirring for 24 h the mixture was diluted with water (50 mL) and the aqueous phase was extracted with Et₂O (5 x 150 mL). The combined organic layers were washed with brine (150 mL) and dried over NaSO₄. The solvent was evaporated and purification of the crude product by column chromatography (PE:EA = 95:5) yielded compound **2a** (21.14 g, 120.0 mmol, 92%) as a red-orange oil.

¹H NMR (400 MHz, CDCl₃): δ = 7.37 – 7.35 (m, 2H), 7.28 – 7.24 (m, 2H), 7.08 – 7.04 (m, 1H), 3.74 (s, 3H).

The analytical data were in accordance with the literature.[6]

methyl 2-diazo-2-(4-nitrophenyl)acetate (2b)

2b
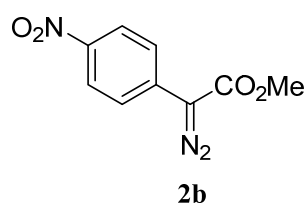
DBU (3.51 g, 23.1 mmol, 1.5 equiv) was added dropwise to a solution of methyl 2-(4-nitrophenyl)acetate (3.00 g, 15.4 mmol, 1.0 equiv) and TsN$_3$ **4** (4.55 g, 23.1 mmol, 1.5 equiv) in dry MeCN (150 mL) at room temperature under nitrogen atmosphere. After stirring for 24 h the mixture was diluted with water (50 mL) and the aqueous phase was extracted with Et$_2$O (3 x 50 mL). The combined organic layers were washed with brine (50 mL) and dried over MgSO$_4$. The solvent was evaporated and purification of the crude product by column chromatography (PE:EA = 95:5) yielded compound **2b** (3.00 g, 13.6 mmol, 88%) as a yellow solid.

^{1}H NMR (400 MHz, CDCl$_3$): δ = 8.24 – 8.21 (m, 2H), 7.67 – 7.65 (m, 2H), 3.90 (s, 3H).

The analytical data were in accordance with the literature.[7]

methyl 2-(4-chlorophenyl)-2-diazoacetate (2c)

2c
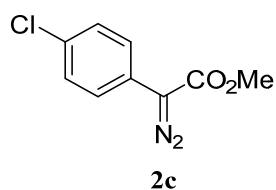
DBU (3.41 g, 22.4 mmol, 1.5 equiv) was added dropwise to a solution of methyl 2-(4-chlorophenyl)acetate (2.75 g, 14.9 mmol, 1.0 equiv) and TsN$_3$ **4** (4.42 g, 22.4 mmol, 1.5 equiv) in dry MeCN (150 mL) at room temperature under nitrogen atmosphere. After stirring for 24 h the mixture was diluted with water (50 mL) and the aqueous phase was extracted with Et$_2$O (3 x 50 mL). The combined organic layers were washed with brine (50 mL) and dried over MgSO$_4$. The solvent was evaporated and purification by chromatography (PE:EA = 95:5) yielded compound **2c** (2.73 g, 13.0 mmol, 87%) as an orange solid.

^{1}H NMR (400 MHz, CDCl$_3$): δ = 7.33 – 7.31 (m, 2H), 7.26 – 7.24 (m, 2H), 3.77 (s, 3H).

The analytical data were in accordance with the literature.[6]

methyl 2-diazo-2-(4-methoxyphenyl)acetate (2d)

2d
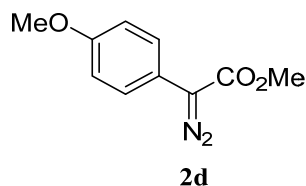
DBU (4.69 g, 30.8 mmol, 1.5 equiv) was added dropwise to a solution of methyl 2-(4-methoxyphenyl)acetate (3.69 g, 20.5 mmol, 1.0 equiv) and TsN$_3$ **4** (6.07 g, 30.8 mmol, 1.5 equiv) in dry MeCN (150 mL) at room temperature under nitrogen atmosphere. After stirring for 24 h the mixture was diluted with water (50 mL) and the aqueous phase was extracted with Et$_2$O (3 x 50 mL). The combined organic layers were washed with brine (50 mL) and dried over MgSO$_4$. The solvent was evaporated and purification by chromatography (PE:EA = 95:5) yielded compound **2d** (3.42 g, 16.6 mmol, 81%) as a red solid.

^{1}H NMR (400 MHz, CDCl$_3$): δ = 7.38 – 7.25 (m, 2H), 7.28 – 7.24 (m, 2H), 7.08 – 7.04 (m, 1H), 3.74 (s, 3H), 3.70 (s, 3H).

The analytical data were in accordance with the literature.[6]

4.2 Photoinduced Cyclopropanation of Heterocycles in Flow

General Procedure (GP) for the Photoinduced Cyclopropanation of Heterocycles in Flow:
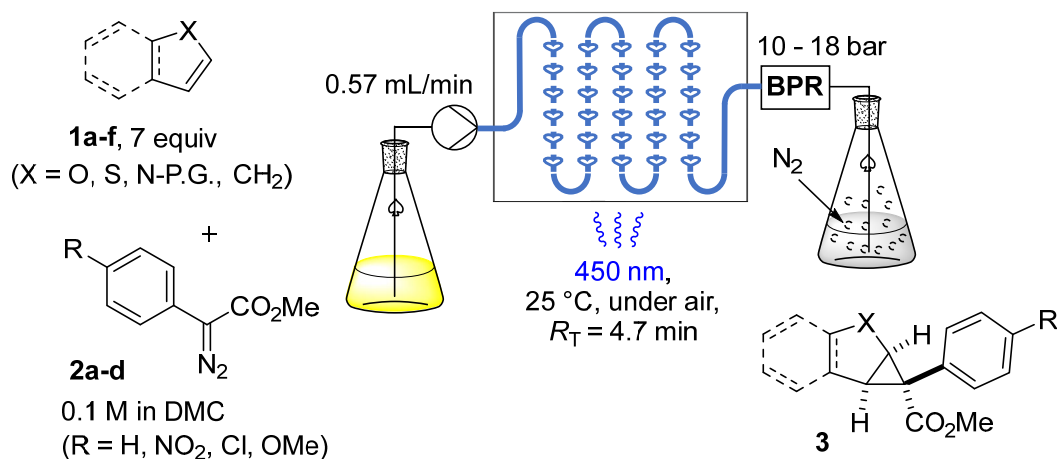
Under air, diazoacetate **2** (1 equiv, 0.1 M), 1,3,5-trimethoxybenzene (0.1 equiv, 0.01M, for quantitative NMR-analysis) and heterocycle **1** (from 7 equiv, 0.7 M) were dissolved in DMC (DCM and DCE during optimization) to form a homogenous feedstock. From this point, the feedstock was kept cool either in the fridge (for storage) or by an ice bath (during experiments) and kept in the dark with foil shielding. Before pumping the solution through the system, the reactor was flushed with the used solvent and the wavelength was set to 450 nm. Each sample was collected after conditioning the reactor to the set conditions (if not otherwise specified, under the optimal conditions as defined by the DoE study: R_T = 4.7 min, I_L = 100%, T = 25°C). The volume of each sample was measured and the solvent was evaporated under reduced pressure. Purification was performed by column chromatography using petroleum ether/ ethyl acetate (PE : EA = 19:1, 9:1 + 20% triethylamine) as eluent.

methyl (1S,5S,6R)-6-phenyl-2-oxabicyclo[3.1.0]hex-3-ene-6-carboxylate (3aa)

*As reactive intermediates for further synthetic transformations, the hazards of all compounds in family **3** are unknown and compounds should be treated as toxic until data are available.*

3aa
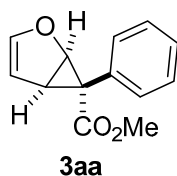
8.85 mmol scale run at higher selectivity:

Cyclopropanation of furan (**1a**) was performed according to the GP. Furan (**1a**) (4.77 g, 70 mmol, 7 equiv) and diazo compound **2a** (1.76 g, 10 mmol, 1 equiv) were dissolved in 100 mL DMC. After performing the flow reaction for 2.4 h (= after pumping 8.21 mmol of the substrate through the reactor system), the solvent was evaporated at reduced pressure and 1.46 g (6.73 mmol, 82%, 608 mg/h) of the colorless crystalline product **3aa** was isolated by chromatography.

65 mmol scale run at higher productivity:

Under air, diazoacetate **2a** (14.0 g, 0.080 mol, 1 equiv) and furan (**1a**) (37.9 g ,0.556 mol, 7 equiv) were dissolved in 265 mL DMC to form a homogenous feedstock. From this point, the

feedstock was kept cool either in the fridge (for storage) or by an ice bath (during experiments) and kept in the dark with foil shielding. Before pumping the solution through the system, the reactor was flushed with the used solvent. The sample was collected after conditioning the reactor to the set conditions (R_T = 4.7 min, I_L = 100%, T = 25°C). After running the experiment for 7.4 h (= after pumping 0.075 mol of the substrate through the reactor system), the volume was measured, the solvent evaporated and the product **3aa** was isolated by column chromatography using petroleum ether/ethyl acetate (PE : EA = 19:1, 9:1 + 20% triethylamine) as eluent to obtain 9.89 g (0.046 mol, 60%, 1331 mg/h).

Gram-scale batch reaction comparison

Under air, diazoacetate **2a** (3.3 g, 0.019 mol, 1 eq) and furan (**1a**) (9.1 g, 0.133 mol, 7 equiv) were dissolved in 180 mL DMC to form a homogenous solution. The solution was transferred into the large-scale batch reactor and was irradiated at 455 nm. After running the experiment for 5 h, the solvent was evaporated and the product **3aa** was isolated by column chromatography (PE : EA = 19:1, 9:1 + 20% triethylamine) to obtain 2.08 g (9.60 mmol, 51%).

m.p. 72-73 °C

R$_f$: (PE:EA =5:1) = 0.35.

^{1}H NMR (400 MHz, CDCl$_3$): δ 7.28 – 7.24 (m, 3H), 7.19 – 7.17 (m, 2H), 5.91 (dd, J = 2.6, 0.8 Hz, 1H), 5.22 (t, J = 2.6, Hz, 1H), 5.13 (dd, J = 5.6, 0.8 Hz, 1H), 3.61 (s, 3H), 3.30 (dd, J = 5.6, 2.6 Hz, 1H)

^{13}C NMR (101 MHz, CDCl$_3$): δ = 174, 147.4, 132.8, 130.8, 127.9, 127.6, 104.1, 70.9, 52.6, 39.4, 27.9

HR MS (EI): calc. for C$_{13}$H$_{12}$O$_3$ (M) $^{\bullet+}$, m/z = 216.0781; found 216.0782.

IR (ATR): ν 3105, 3001, 2952, 1700, 1592, 1431, 1308, 1252, 1148, 1051, 1018, 977, 951, 835, 723 cm^{-1}.

The analytical data were in accordance with the literature.[8]

dimethyl (1S,5S,6R)-6-phenyl-2-oxabicyclo[3.1.0]hex-3-ene-3,6-dicarboxylate (3ba)

3ba
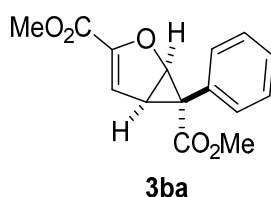
According to GP, methyl furan-2-carboxylate (**1b**) (836.8 mg, 6.6 mmol, 7 equiv) and methyl 2-diazo-2-phenylacetate (**2a**) (167 mg, 1 mmol, 1 equiv) were dissolved in DMC (10 mL). The solution was pumped through the reactor and collected. Purification via chromatography yielded 135.2 mg of the target compound **3ba** (0.52 mmol, 52%) as a colorless solid.

m.p. 103-104 °C

R$_f$ (PE:EA = 5:1) = 0.25.

^{1}H NMR (400 MHz, CDCl$_3$): δ = δ 7.27 − 7.19 (m, 5H), 6.11 (d, J = 3.0 Hz, 1H), 5.23 (d, J = 5.4 Hz, 1H), 3.64 (s, 3H), 3.61 (s, 3H), 3.37 (dd, J = 5.4, 3.0 Hz, 1H);

^{13}C NMR (101 MHz, CDCl$_3$): δ = : δ 173.3, 159.0, 149.0 , 132.4, 129.7, 128.2, 127.9, 114.2, 71.2, 53.0, 52.2, 39.6, 28.7

HR MS (EI): calcd. for C$_{15}$H$_{14}$O$_5$ (M) $^{\bullet+}$, m/z = 274.0836; found 274.0833.

IR (ATR): ν 2952, 1737, 1711, 1607, 1435, 1252, 1210, 1189, 1148, 1111, 1044, 954, 738, 701 cm^{-1}.

The analytical data were in accordance with the literature.[8]

methyl (1R,1aS,6bS)-1-phenyl-1a,6b-dihydro-1H-cyclopropa[b]benzofuran-1-carboxylate (3ca)

3ca
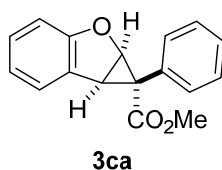
According to GP, 2,3-benzofuran (**1c**) (454.4 mg, 3.9 mmol, 7 equiv) and methyl 2-diazo-2-phenylacetate (**2a**) (96.8 mg, 0.6 mmol, 1 equiv) were dissolved in DMC (6 mL). The solution was pumped through the reactor and collected. Purification via chromatography yielded 71.7 mg of the target compound **3ca** (0.3 mmol, 49%) as a colorless solid.

m.p. 122-123 °C

R$_f$ (PE:EA = 5:1) = 0.41.

**^{1}H NMR** (400 MHz, CDCl$_3$): δ = 7.35 (dd, J = 7.4 Hz, 1.4 Hz, 1H), 7.07 (s, 5H), 6.90 (td, J = 7.8 Hz, J = 1.4 Hz, 1H), 6.80 (td, J = 7.4 Hz, 1.0 Hz, 1H), 6.45 (d, J = 7.1 Hz, 1H), 5.36 (d, J = 5.5 Hz, 1H), 3.79 (d, J = 5.5 Hz, 1H), 3.67 (s, 3H).

^{13}C NMR (101 MHz, CDCl$_3$): δ = 173.5, 159.6, 132.6, 129.7, 128.1, 127.7, 127.3, 126.6, 125.2, 121.3, 109.8, 70.6, 52.9, 37.5, 31.1.

HR MS (EI): calcd. for C$_{17}$H$_{14}$O$_3$ (M)$^{•+}$, m/z = 266.0938; found 266.0937.

IR (ATR): ν 2952, 1703, 1435, 1238, 1155, 1029, 854, 752, 693 cm^{-1}.

The analytical data were in accordance with the literature.[8]

methyl (1S,5S,6R)-6-phenyl-2-oxabicyclo[3.1.0]hexane-6-carboxylate (3da)
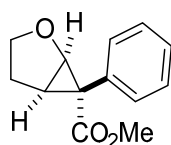
3da

According to GP, 2,3-dihydrofuran (**1d**) (981 mg, 14.0 mmol, 7 equiv) and methyl 2-diazo-2-phenylacetate (**2a**) (352 mg, 2 mmol, 1 equiv) were dissolved in DMC (20 mL). The solution was pumped through the reactor and collected for 20 min (= 11.4 mL). Purification via chromatography yielded 152.1 mg of the target compound **3da** (0.70 mmol, 61 %) as a colorless solid.

^{1}H NMR (300 MHz, CDCl$_3$): δ = 7.40 – 7.29 (m, 5H), 4.50 (d, J = 5.7 Hz, 1H), 3.77 (ddd, J = 10.0, 8.3, 3.6 Hz, 1H), 3.57 (s, 3H), 2.65 (t, J = 5.7 Hz, 1H), 2.42 – 2.31 (m, 1H), 2.29 – 2.18 (m, 1H), 1.89 – 1.81 (m, 1H).

^{13}C NMR (75 MHz, CDCl$_3$): δ = 172.1, 132.3, 131.6 (2x), 128.6 (2x), 127.6, 70.2, 70.1, 52.4, 38.1, 32.5, 26.3.

The analytical data were in accordance with the literature.[9]

methyl 7-phenyl-2-oxabicyclo[4.1.0]heptane-7-carboxylate (3ea)

3ea
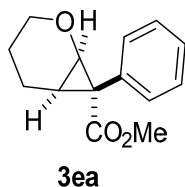
According to GP, 3,4-dihydro-*2H*-pyran (**1e**) (1177,7 mg, 14 mmol, 7 equiv) and methyl 2-diazo-2-phenylacetate (**2a**) (352 mg, 2 mmol, 1 equiv) were dissolved in DMC (20 mL). The solution was pumped through the reactor and collected for 20 min (= 11.4 mL). Purification via chromatography yielded 137 mg of the target compound **3ea** (0.59 mmol, 52%) as a colorless solid.

^{1}H NMR (300 MHz, CDCl$_3$): δ 7.40 – 7.27 (m, 5H), 4.21 (d, J = 7.5 Hz, 1H), 3.56 (s, 3H), 3.44 – 3.38 (m, 1H), 3.30 (ddd, J = 12.0, 10.6, 2.0 Hz, 1H), 2.16 (td, J = 7.2, 1.2 Hz, 1H), 2.01 (ddt, J = 14.0, 11.2, 6.9 Hz, 1H), 1.92 – 1.84 (m, 1H), 1.08 – 0.98 (m, 1H), 0.38 – 0.22 (m, 1H).

^{13}C NMR (101 MHz, CDCl$_3$): δ 173.9, 133.4, 132.7 (2x), 128.2 (2x), 127.2, 64.6, 62.3, 52.5, 35.0, 25.5, 21.3, 17.6.

The analytical data were in accordance with the literature.[9]

methyl (1S,5R,6S)-6-phenylbicyclo[3.1.0]hex-2-ene-6-carboxylate (3fa)

3fa
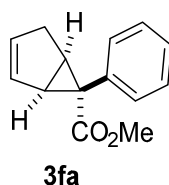
According to GP, freshly destilled cyclopentadiene (**1f**) (925 mg, 14 mmol, 7 equiv) and methyl 2-diazo-2-phenylacetate (**2a**) (352 mg, 2 mmol, 1 equiv) were dissolved in DMC (20 mL). The solution was pumped through the reactor and collected for 20 min (= 11.4 mL). Purification via chromatography yielded 173.4 mg of the target compound **3fa** (0.81 mmol, 71%) as a colorless solid.

^{1}H NMR (300 MHz, CDCl$_3$): δ 7.21 – 7.23 (m, 3H), 7.13 – 7.10 (m, 2H), 5.78 – 5.74 (m, 1H), 5.23 – 5.20 (m, 1H), 3.59 (s, 3H), 2.96 – 2.92 (m, 1H), 2.69 – 2.62 (m, 2H), 2.13 – 2.04 (m, 1H).

^{13}C NMR (101 MHz, CDCl$_3$): δ 174.5, 133.1, 133.0 (2x), 132.9, 129.7, 127.7 (2x), 126.8, 52.5, 40.9, 37.9, 34.2, 32.4.

The analytical data were in accordance with the literature.[10]

Methyl (1S,5S,6R)-6-phenyl-2-tosyl-2-azabicyclo[3.1.0]hex-3-ene-6-carboxylate (3ga)

3ga
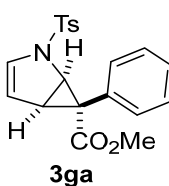
According to GP, *tert*-butyl 1-pyrrolecarboxylate (**1g**) (3097.8 mg, 14 mmol, 7 equiv) and methyl 2-diazo-2-phenylacetate (**2a**) (352 mg, 2 mmol, 1 equiv) were dissolved in DMC (20 mL). The solution was pumped through the reactor and collected for 20 min (= 11.4 mL). Purification via chromatography yielded 205.9 mg of the target compound **3ga** (0.35 mmol, 51%) as a colorless solid.

^{1}H NMR (400 MHz, CDCl$_3$): δ = 7.71 (d, *J* = 8.3 Hz, 2H), 7.33 (d, *J* = 8.5 Hz, 2H), 7.27 – 7.24 (m, 3H), 7.21 – 7.19 (m, 2H), 5.95 (dd, *J* = 3.9 Hz, 1.5 Hz, 1H), 5.28 (dd, *J* = 3.9 Hz, 2.5 Hz, 1H), 4.53

(dd, *J* = 6.5 Hz, 1.4 Hz, 1H), 3.60 (s, 3H), 3.14 (dd, *J* = 6.5 Hz, 2.5 Hz, 1H), 2.45 (s, 3H), 2.45 (s, 3H).

¹³C NMR (101 MHz, CDCl₃): δ = 173.7, 144.5, 135.0, 132.6 (2x), 130.9, 130.5, 130.1 (2x), 127.9, 127.5, 127.3, 127.0, 111.4 (2x), 52.9, 52.3, 38.8, 28.1, 21.7.

The analytical data were in accordance with the literature.[11]

2-(*tert*-butyl)   methyl-(1S,5S,6R)-6-phenyl-2-azabicyclo[3.1.0]hex-3-ene-2,6-dicarboxylate (3ha)

3ha
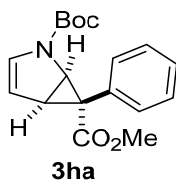
According to GP, *tert*-butyl 1-pyrrolecarboxylate (**1h**) (813.6 mg, 4.9 mmol, 7 equiv) and methyl 2-diazo-2-phenylacetate (**2a**) (122.5 mg, 0.7 mmol, 1 equiv) were dissolved in DMC (7 mL). The solution was pumped through the reactor and collected. Purification via chromatography yielded 111.2 mg of the target compound **3ha** (0.35 mmol, 51%) as a colorless solid.

m.p. 122-125 °C

R*f* (PE:EA = 9:1) = 0.44.

¹H NMR (400 MHz, CDCl₃) 2 rotamers: δ = 7.30 – 7.25 (m, 3H), 7.17 – 7.11 (m, 2H), 6.15 (d, *J* = 4.0 Hz, 0.4H), 5.99 (d, *J* = 4.4 Hz, 0.6H), 5.21 (dd, *J* = 4.0 Hz, 2.7 Hz, 0.4H), 5.14 (dd, *J* = 4.0 Hz, 2.7 Hz, 0.6H), 4.72 (d, *J* = 7.9 Hz, 0.6H), 4.62 (d, *J* = 7.9 Hz, 0.4H), 3.65 (s, 1.2H), 3.62 (s, 1.8H), 3.35 – 3.32 (m, 1H), 1.61 (s, 3.6 H), 1.47 (s, 5.4H)

¹³C NMR (101 MHz, CDCl₃) 2 rotamers: δ = 174.2, 173.9, 151.4, 151.3, 132.8, 132.5, 131.3, 131.1, 130.9, 130.6, 128.0, 127.9, 127.5, 127.4, 107.4 (x2), 82.0, 81.7, 52.7, 52.6, 49.5, 49.4, 39.7, 38.4, 29.8, 29.4, 28.5, 28.3.

HR MS (ESI): calcd. for $C_{18}H_{21}NO_4$ (M+H)⁺, m/z = 316.1543; found 316.1544.

IR (ATR): ν 3116, 2982, 1700, 1592, 1435, 1402, 1364, 1241, 1133, 954, 704 cm^{-1}.

The analytical data were in accordance with the literature.[1]

dimethyl 7-phenyl-2-azabicyclo[4.1.0]heptane-2,7-dicarboxylate (3ia)

3ia
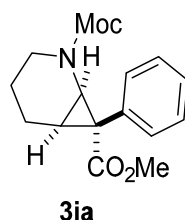
According to GP, methyl 3,4-dihydro-*2H*-pyridine-1-carboxylate (**1i**) (1779 mg, 14 mmol, 7 equiv) and methyl 2-diazo-2-phenylacetate (**2a**) (352 mg, 2 mmol, 1 equiv) were dissolved in DMC (20 mL). The solution was pumped through the reactor and collected for 20 min (= 11.4 mL). Purification via chromatography yielded 185.3 mg of the target compound **3ia** (0.65 mmol, 57%) as a colorless solid.

**m.p.** 151-154 °C

R$_f$ (PE:EA = 4:1) = 0.51.

^{1}H NMR (300 MHz, CDCl$_3$) 2 rotamers: δ 7.31 – 7.09 (m, 5H), 3.83 (s, 1.8H), 3.75 (s, 1.2H), 3.73 (s, 2H, both rotamers), 3.55 (s, 1.9H), 3.52 (s, 1.1H), 3.23 – 3.15 (m, 0.6H), 3.13 – 3.05 (m, 0.4H), 2.76 – 2.66 (m, 1H, both rotamers), 2.37 – 2.24 (m, 1H, both rotamers), 1.96 – 1.73 (m, 2H, both rotamers), 1.19 – 1.11 (m, 1H, both rotamers), 0.42 – 0.28 (m, 1H, both rotamers).

^{13}C NMR (101 MHz, CDCl$_3$) rotamer 1 (rotamer 2): δ = 173.9 (173.7), 157.7 (157.5), 133.4 (133.2), 138.8 (138.5) (2x), 128.7 (128.5) (2x), 127.6 (127.4), 53.1 (53.0), 57.7 (57.7), 42.6 (42.3), 41.5 (41.1), 34.9 (34.7), 25.1 (24.8), 21.1 (20.9), 18.7 (18.6).

HR MS (EI): calcd. for C$_{16}$H$_{19}$NO$_4$ (M) $^{\bullet+}$, m/z = 289.1309; found 289.1307.

IR (ATR): ν 2952, 1685, 1439, 1383, 1245, 1197, 1103, 962, 772, 705 cm^{-1}.

2-(tert-butyl) 1-methyl-(1R,1aS,6bS)-1-phenyl-1a,6b-dihydrocyclopropa[b]indole-1,2(1H)-dicarboxylate (3ja)
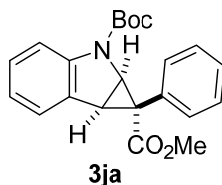
According to GP, *tert*-butyl 1-indolecarboxylate (**1j**) (1.833 g, 8.4 mmol, 7 equiv) and methyl 2-diazo-2-phenylacetate (**2a**) (212.3 mg, 1.2 mmol, 1 equiv) were dissolved in DMC (11 mL). The solution was pumped through the reactor and collected. Purification via chromatography yielded 246.6 mg of the target compound **3ja** (0.7 mmol, 56%) as a yellowish oil.

m.p. 130-134°C

R$_f$ (PE:EA = 9:1) = 0.47.

^{1}H NMR (400 MHz, CDCl$_3$) 2 rotamers: δ = 7.43 (d, *J* = 8.0 Hz, 1H), 7.38 (d, *J* = 7.2 Hz, 1H), 7.06-7.04 (m, 3H), 7.01-6.96 (m, 3H), 6.92-6.88 (m, 1H), 4.97 (d, *J* = 6.8 Hz, 0.5H), 4.86 (d, *J* = 6.8 Hz, 0.5H), 3.73 (t, *J* = 6.6 Hz, 1H), 3.68 (d, *J* = 10.3, 1.5Hz), 3.65 (s, 1.5H), 1.65 (s, 4.5H), 1.59 (s, 4.5H).

^{13}C NMR (101 MHz, CDCl$_3$): δ = 173.7, 173.5, 153.0, 151.8, 142.5, 141.4, 132.4, 132.1, 130.5, 130.4, 129.3, 128.5, 128.0, 127.8, 127.7, 127.4, 127.3, 125.7, 125.2, 122.5, 122.4, 114.7, 114.5, 82.7, 82.0, 52.9, 52.8, 50.8, 50.7, 35.6, 34.8, 32.2, 31.9, 28.6, 28.4.

HR MS (ESI): calcd. for C$_{22}$H$_{23}$NO$_4$ (M+H)$^+$, m/z = 366.1700; found 366.1696.

IR (ATR): ν 2974, 1707, 1476, 1379, 1320, 1245, 1152, 1005, 746, 701 cm^{-1}.

The analytical data were in accordance with the literature.[1]

2-tert-butyl 1-methyl 5-fluoro-1-phenyl-1,6b-dihydrocyclopropa[b]indole-1,2(1aH)-dicarboxylate (3ka)

3ka
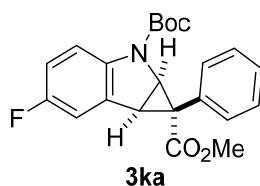
According to GP, tert-butyl 5-fluoroindole-1-carboxylate (**1k**) (1.600 g, 6.8 mmol, 7 equiv) and methyl 2-diazo-2-phenylacetate (**2a**) (0.171 mg, 0.97 mmol, 1 equiv) were dissolved in DMC (9.7 mL). The solution was pumped through the reactor and collected. Purification via chromatography yielded 212 mg of the target compound **3ka** (0.55 mmol, 57%) as a yellowish oil.

¹H NMR (300 MHz, CDCl₃) 2 rotamers: δ = 7.39 – 7.34 (m, 1H), 7.10 – 7.07 (m, 4H), 6.97 – 6.94 (m, 2H), 6.71 – 6.62 (m, 1H), 4.97 (d, *J* = 6.8 Hz, 0.4H), 4.86 (d, *J* = 6.8 Hz, 0.6H), 3.73 – 3.65 (m, 4H), 1.64 (s, 5H), 1.57 (s, 4H).

¹³C NMR (101 MHz, CDCl₃): δ = 173.5, 173.2, 159.9, 157.5, 152.7, 151.7, 138.7, 137.7, 132.3, 132.0, 130.2, 128.0, 127.9, 127.6, 127.4, 115.5, 115.4, 115.3, 115.2, 114.7, 114.4, 114.2, 112.8, 112.6, 112.4, 112.2, 82.9, 82.1, 53.0, 52.9, 51.3, 51.1, 35.2, 34.4, 32.4, 32.1, 28.6, 28.4.

¹⁹F NMR (282 MHz, CDCl₃): δ = -121.5, -121.9.

The analytical data were in accordance with the literature.[12]

methyl (1S,1aS,6bR)-1-phenyl-1a,6b-dihydro-1H-benzo[b]cyclopropa[d]thiophene-1-carboxylate (3la)

3la
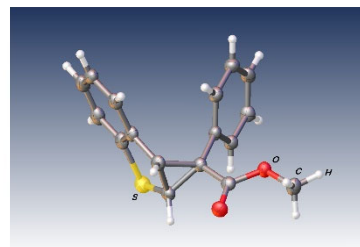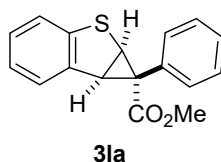
According to GP, 2,3-benzothiophene (**1l**) (2.631 g, 9.3 mmol, 7 equiv) and methyl 2-diazo-2-phenylacetate (**2a**) (234.5 mg, 1.3 mmol, 1 equiv) were dissolved in DMC (11 mL). The solution

was pumped through the reactor and collected. Purification via chromatography yielded 109 mg of the target compound **3la** (0.4 mmol, 29%) as a yellowish solid.

m.p. 179-180 °C

R_f (PE:EA = 9:1) = 0.42.

^{1}H NMR (400 MHz, CDCl$_3$): δ = 7.50 – 7.48 (m, 1H), 7.10 – 7.05 (m, 3H), 7.04 – 7.02 (m, 3H), 6.98 – 6.94 (m, 1H), 6.79 – 6.77 (m, 1H), 4.08 (d, J = 7.8 Hz, 1H), 4.03 (d, J = 7.8 Hz, 1H), 3.66 (s, 3H)

^{13}C NMR (101 MHz, CDCl$_3$): δ = 174.4, 142.9, 136.9, 132.9, 130.8, 127.7, 127.3, 127.2, 126.7, 124.4, 121.7, 53.1, 44.3, 39.9, 31.3

HR MS (EI): calcd. for C$_{17}$H$_{14}$O$_2$S (M)$^{\bullet+}$, m/z = 282.0709; found 282.0703.

IR (ATR): ν 3060, 2952, 1737, 1700, 1435, 1264, 1214, 1205, 1174, 693 cm^{-1}.

The analytical data were in accordance with the literature.[12]

CCDC-Number: 2091948

The crystals were obtained by dissolving the compound in acetone and subsequent slow evaporation of the solvent.

methyl (1S,5S,6R)-6-(4-nitrophenyl)-2-oxabicyclo[3.1.0]hex-3-ene-6-carboxylate (3ab)
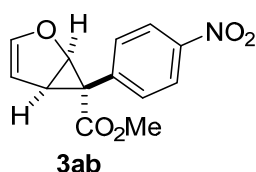
3ab

According to GP but with an residence time of 6.75 min, furan (**1a**) (571.8 mg, 8.4 mmol, 7 equiv) and methyl 2-diazo-2-(4-nitrophenyl)acetate (**2b**) (265.6 mg, 1.2 mmol, 1 equiv) were dissolved in DMC (11.5 mL). The solution was pumped through the reactor and collected. Purification via chromatography yielded 84.6 mg of the target compound **3ab** (0.32 mmol, 27%) as a colorless solid.

m.p. 69 – 73 °C

R_f (PE:EA = 5:1) = 0.39.

1H NMR (300 MHz, CDCl$_3$): δ = 8.15 – 8.12 (m, 2H), 7.38 – 7.33 (m, 2H), 5.91 (dd, *J* = 2.5 Hz, 0.8 Hz, 1H), 5.25 (t, *J* = 2.6 Hz, 1H), 5.20 (dd, *J* =5.6 Hz, 0.8 Hz , 1H), 3.63 (s, 3H), 3.38 (dd, *J* = 5.7, 2.7 Hz, 1H).

13C NMR (75 MHz, CDCl$_3$): δ = 172.5, 147.8, 147.3, 138.6, 133.8 (2x), 123.2 (2x), 104.0, 70.9, 52.9, 39.7, 27.6.

HR MS (EI): calcd. for C$_{12}$H$_{10}$NO$_5$ (M) $^{\bullet+}$, m/z = 261.0632; found 261.0627.

IR (ATR): ν 3109, 2952, 1700, 1592, 1435, 1249, 1144, 1051, 1018, 977, 954, 689 cm^{-1}.

methyl (1R,5R,6S)-6-(4-chlorophenyl)-2-oxabicyclo[3.1.0]hex-3-ene-6-carboxylate (3ac)
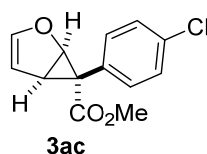
3ac

According to GP but with an residence time of 6.75 min, furan (**1a**) (571.8 mg, 8.4 mmol, 7 equiv) and methyl 2-(4-chlorophenyl)-2-diazoacetate (**2c**) (254.4 mg, 1.2 mmol, 1 equiv) were dissolved in DMC (11.5 mL). The solution was pumped through the reactor and collected. Purification via chromatography yielded 144.4 mg of the target compound **3ac** (0.58 mmol, 48%) as a colorless solid.

m.p. 122 – 125 °C

R$_f$ (PE:EA = 5:1) = 0.31.

1H NMR (400 MHz, CDCl$_3$): δ = 7.29 – 7.28 (m, 2H), 7.15 – 7.12 (m, 2H), 5.95 (d, *J* = 1.8 Hz, 1H), 5.24 (t, *J* = 2.6 Hz, 1H), 5.15 (d, *J* = 5.6, 1H), 3.65 (s, 3H), 3.32 (dd, *J* = 5.6, 2.6, 3.0 Hz, 1H).

13C NMR (101 MHz, CDCl$_3$): δ = 173.6, 147.7, 134.2, 134.2, 133.3, 129.4, 128.3, 128.3, 104.0, 70.9, 52.7, 39.5, 27.3.

HR MS (EI): calcd. for C$_{13}$H$_{11}$O$_3$Cl (M) $^{\bullet+}$, m/z = 250.0391; found 250.0387.

IR (ATR): ν 2952, 1696, 1588, 1498, 1435, 1260, 1144, 1088, 988, 854, 691 cm^{-1}.

methyl (1S,5S,6R)-6-(4-methoxyphenyl)-2-oxabicyclo[3.1.0]hex-3-ene-6-carboxylate (3ad)

3ad
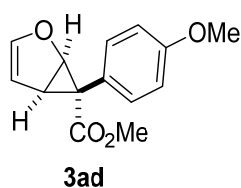
According to GP, furan (**1a**) (281.6 mg, 4.1 mmol, 7 equiv) and methyl 2-diazo-2-(4-methoxyphenyl)acetate (**2d**) (121.8 mg, 0.6 mmol, 1 equiv) were dissolved in DMC (6 mL). The solution was pumped through the reactor and collected. Purification via chromatography yielded 100.4 mg of the target compound **3ad** (0.4 mmol, 69%) as a colorless solid.

m.p. 95 – 97°C

R$_f$ (PE:EA = 5:1) = 0.25.

^{1}H NMR (400 MHz, CDCl$_3$): δ = 7.10 – 7.06 (m, 2H), 7.82 – 7.80 (m, 2H), 5.93 (d, J = 1.8 Hz, 1H), 5.21 (t, J = 2.6 Hz, 1H), 5.11 (d, J = 5.6, 1H), 3.78 (s, 3H), 3.62 (s, 3H), 3.27 (dd, J = 5.6, 2.6 Hz, 1H).

^{13}C NMR (101 MHz, CDCl$_3$): δ = 174.4, 158.8, 147.4, 147.4, 133.9, 133.9, 122.7, 113.4, 104.0, 71.0, 55.2, 52.7, 39.6, 27.2.

HR MS (EI): calcd. for C$_{14}$H$_{14}$O$_4$ (M) $^{\bullet+}$, m/z = 246.0887; found 246.0882.

IR (ATR): ν 3105, 2952, 2840, 1700, 1517, 1431, 1238, 1141, 1017, 977, 950, 716 cm^{-1}.

5 NMR spectra

TsN₃, ¹H NMR (CDCl₃)
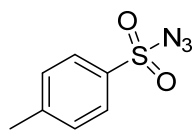
TsN₃
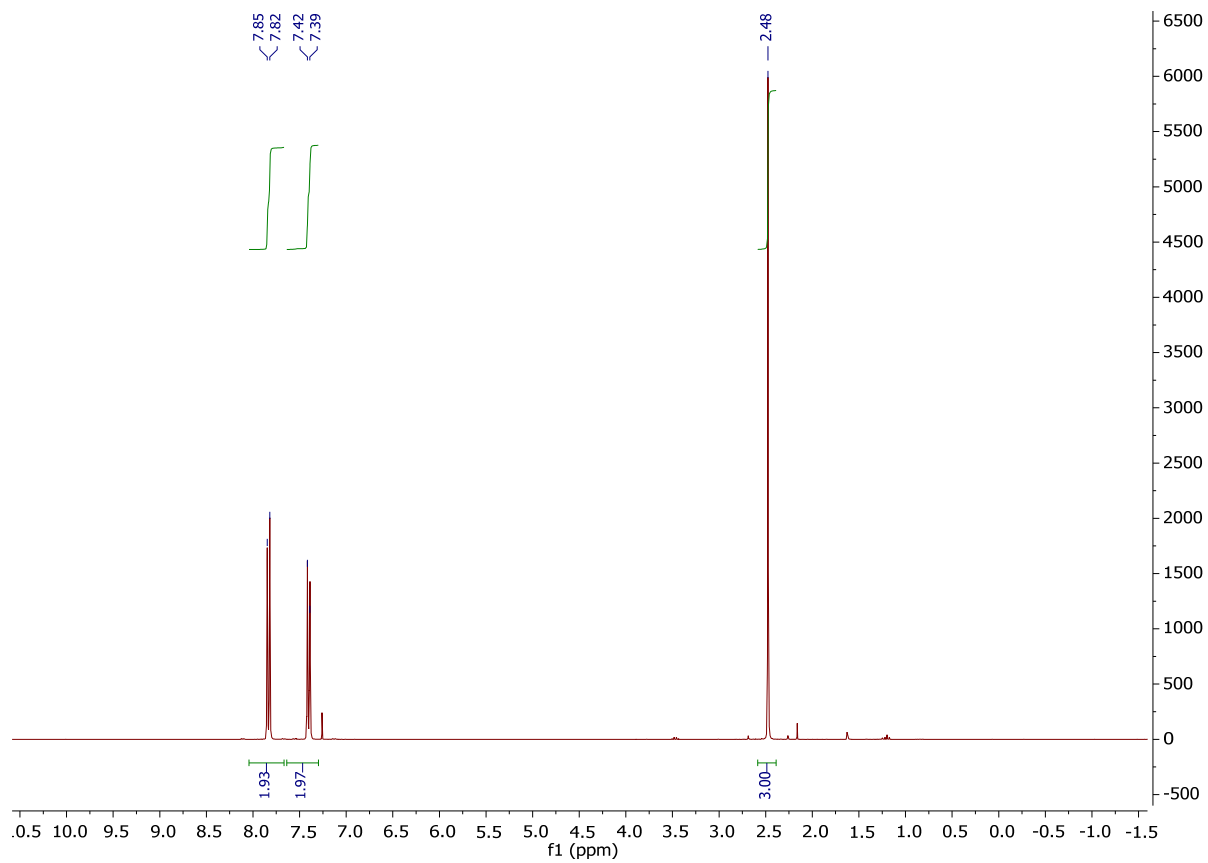
Compound 2a, ¹H NMR (CDCl₃):
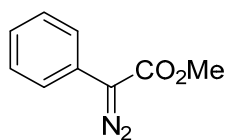
2a
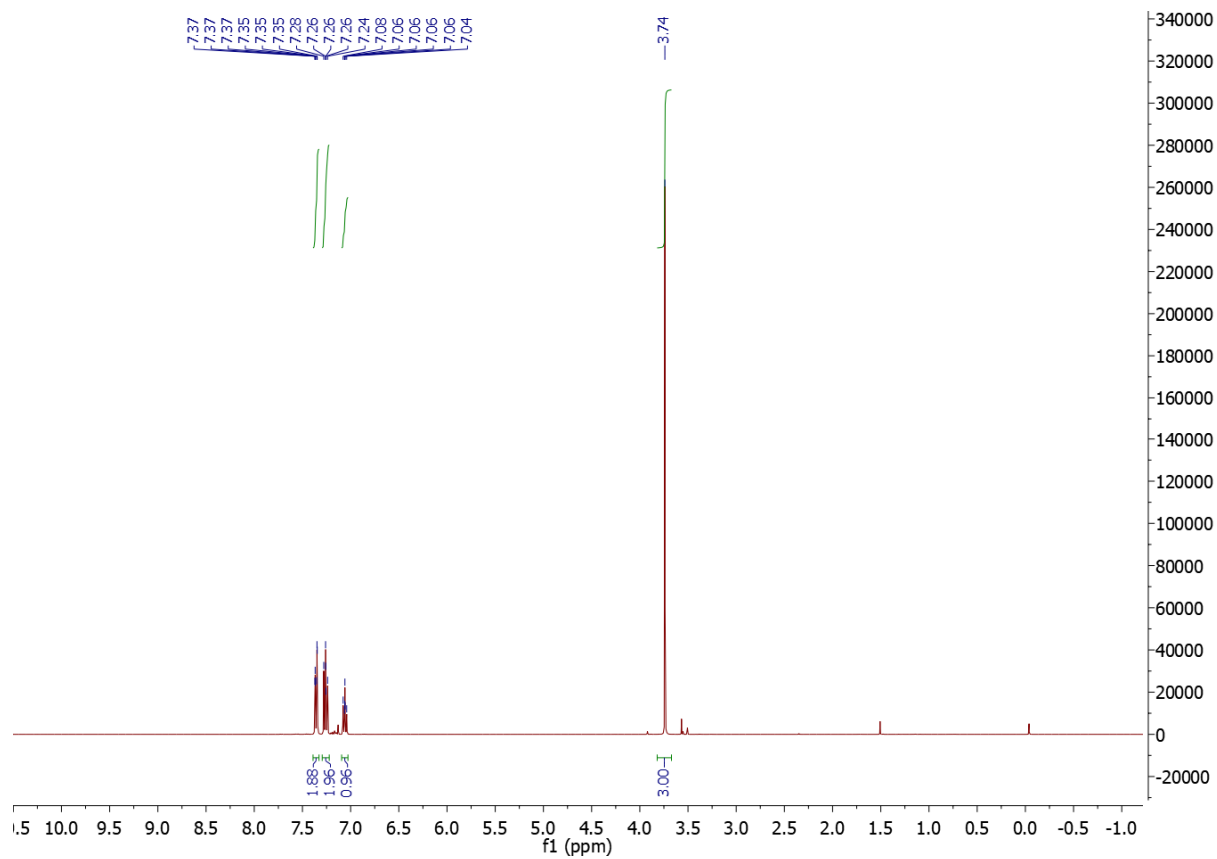
Compound 2b, ^{1}H NMR (CDCl$_3$)
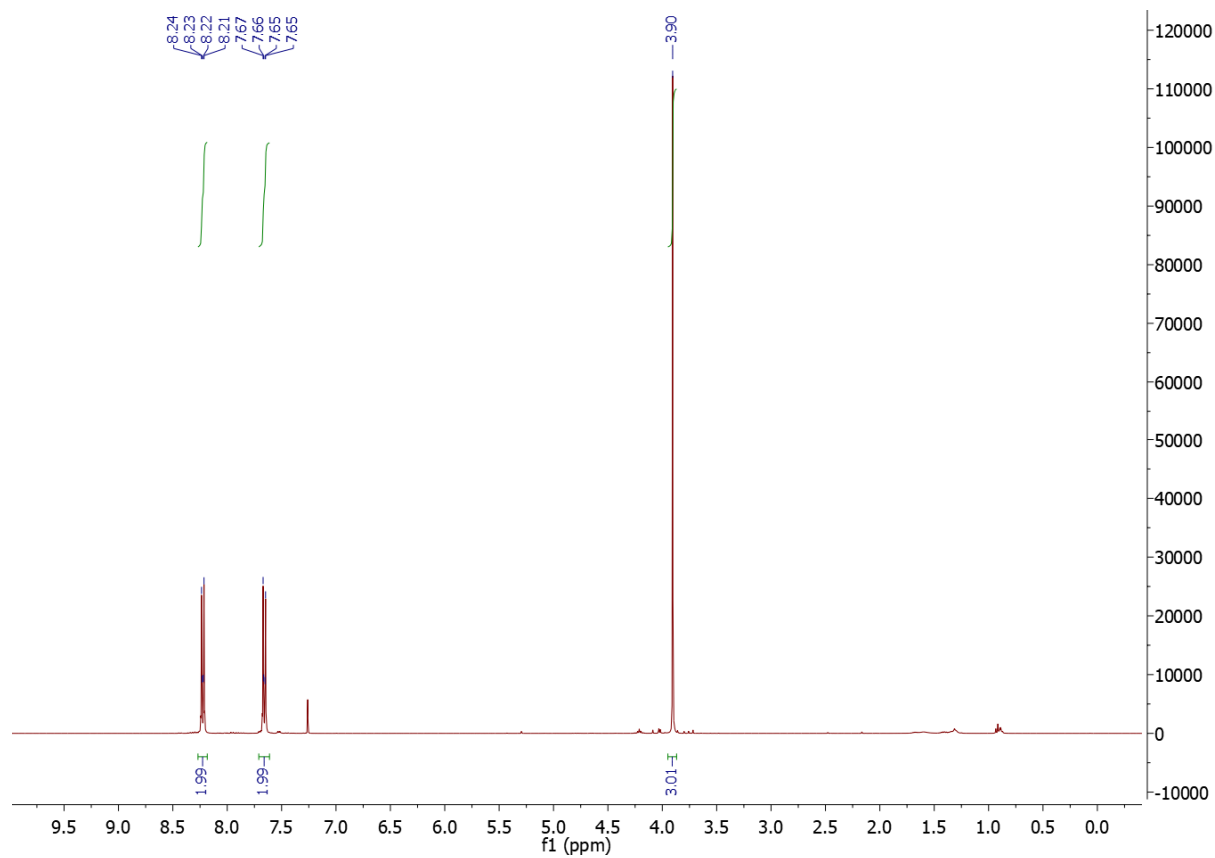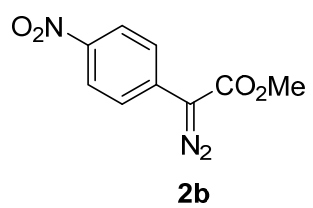
Compound 2c, ^{1}H NMR (CDCl$_3$)

2c

7.33
7.33
7.33
7.32
7.31
7.26
7.25
7.24
7.24
7.24

3.77

1.99
1.99

3.05

f1 (ppm)
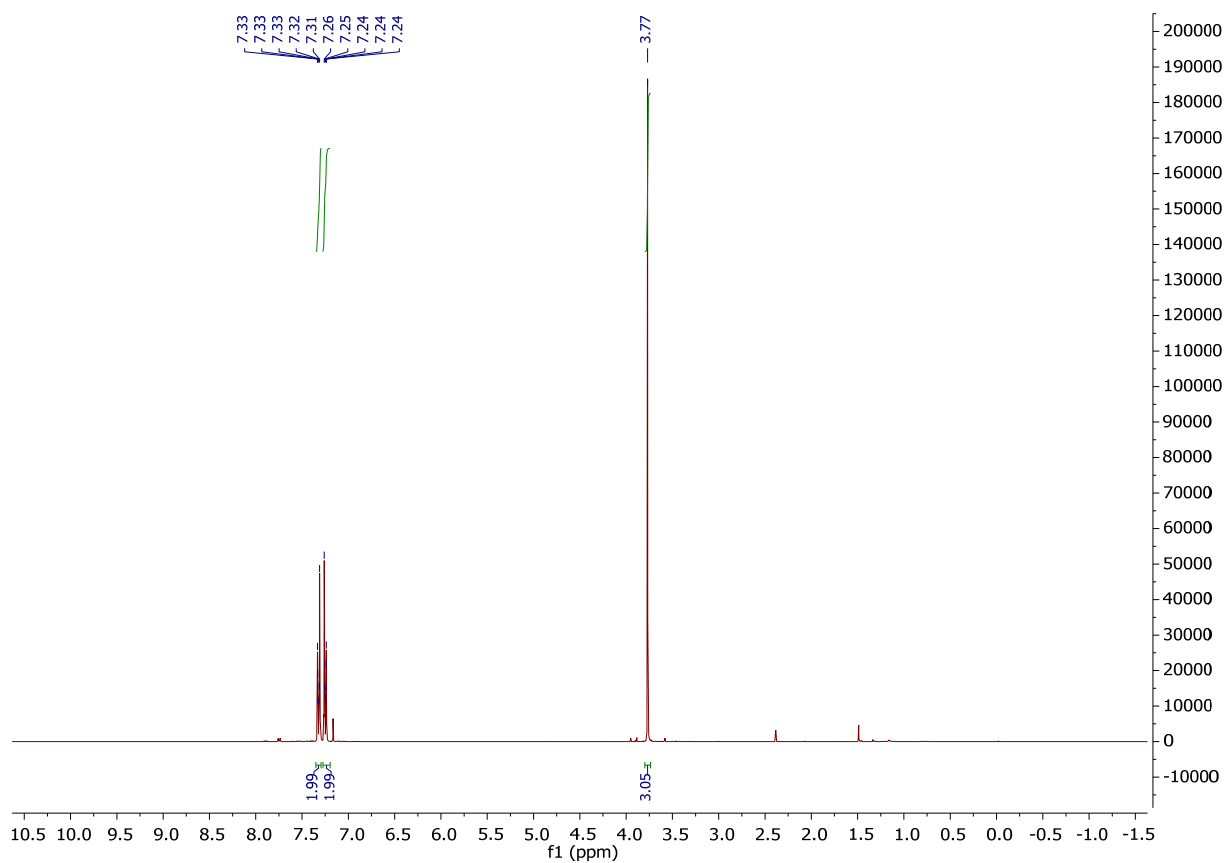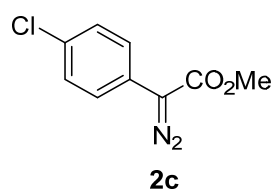
Compound 2d, ¹H NMR (CDCl₃)

MeO— —CO₂Me

N₂

2d
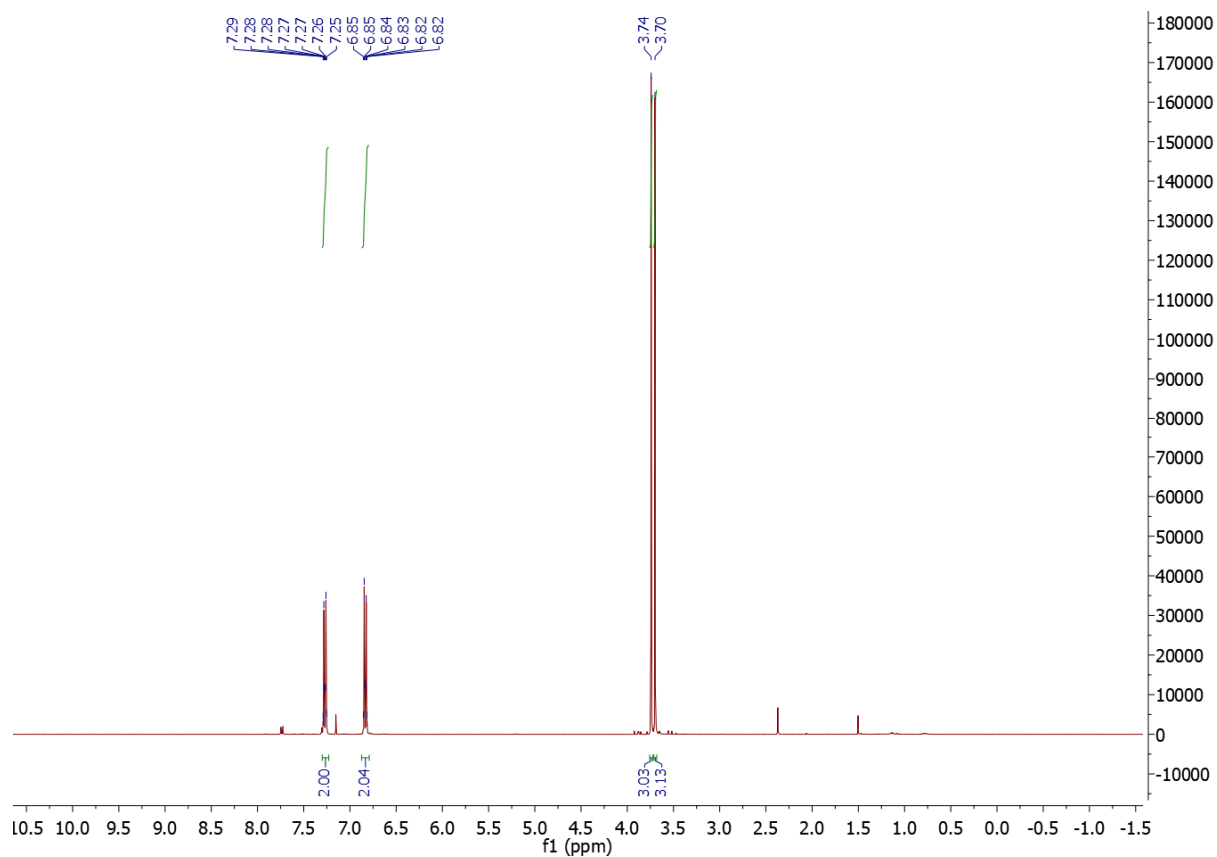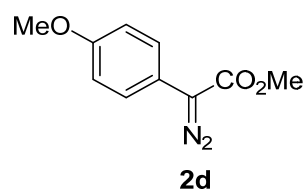
Compound 3aa, ¹H NMR and ¹³C NMR (CDCl₃)

3aa
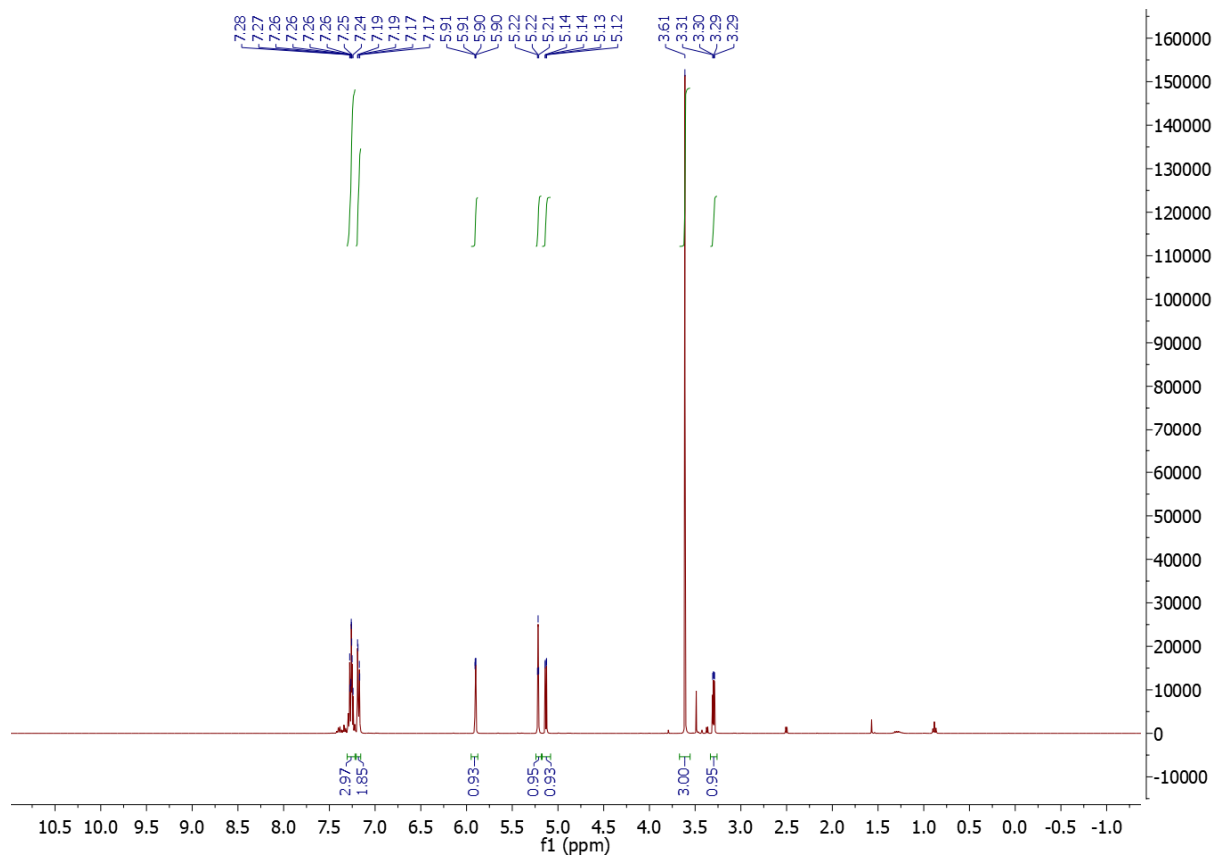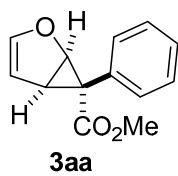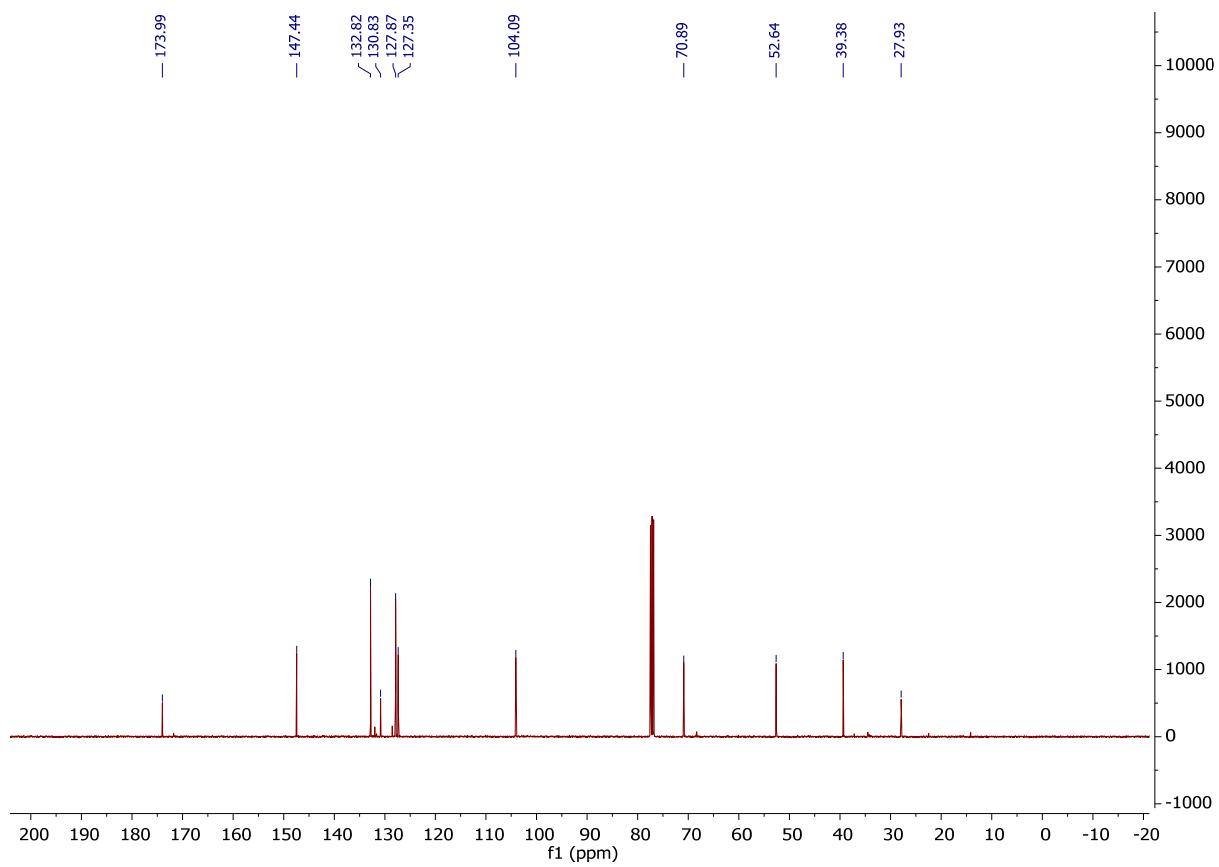
Compound 3ba, ¹H NMR and ¹³C NMR (CDCl₃)
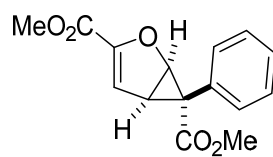
3ba
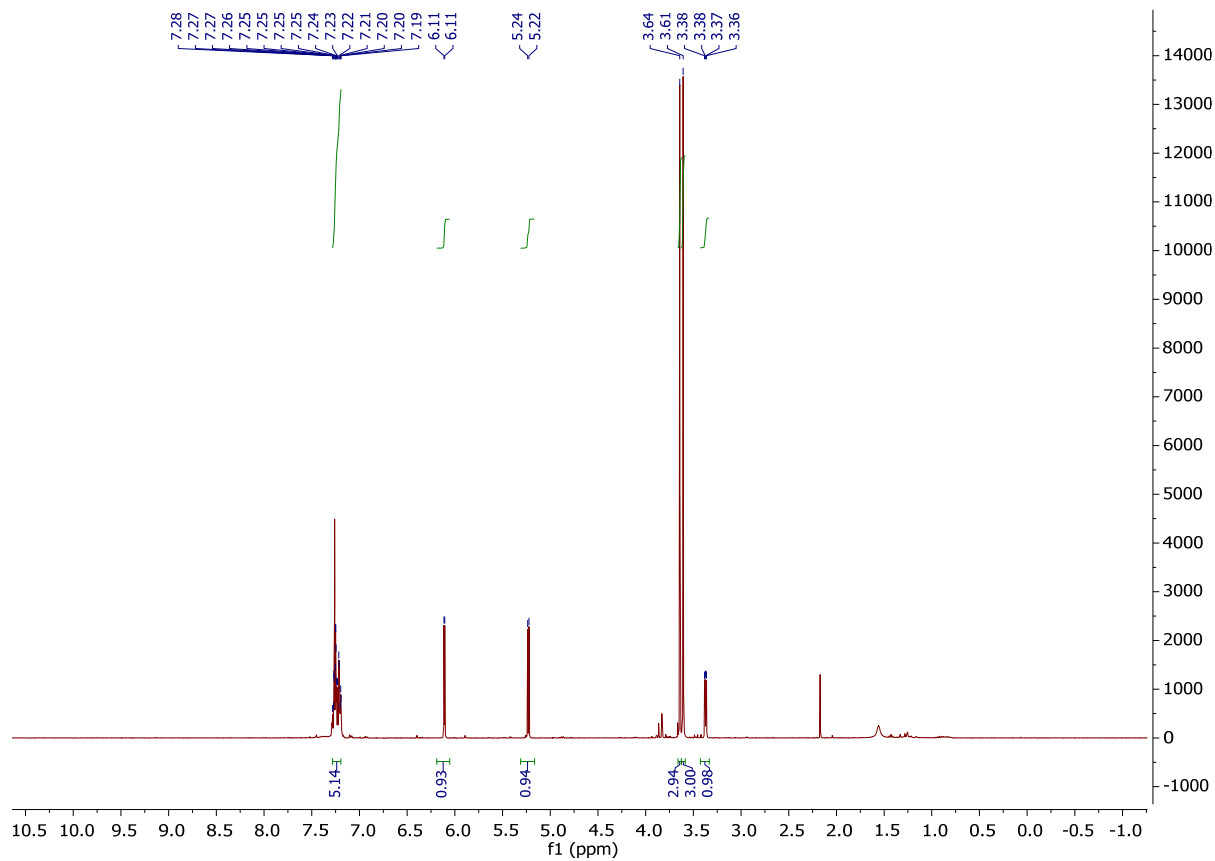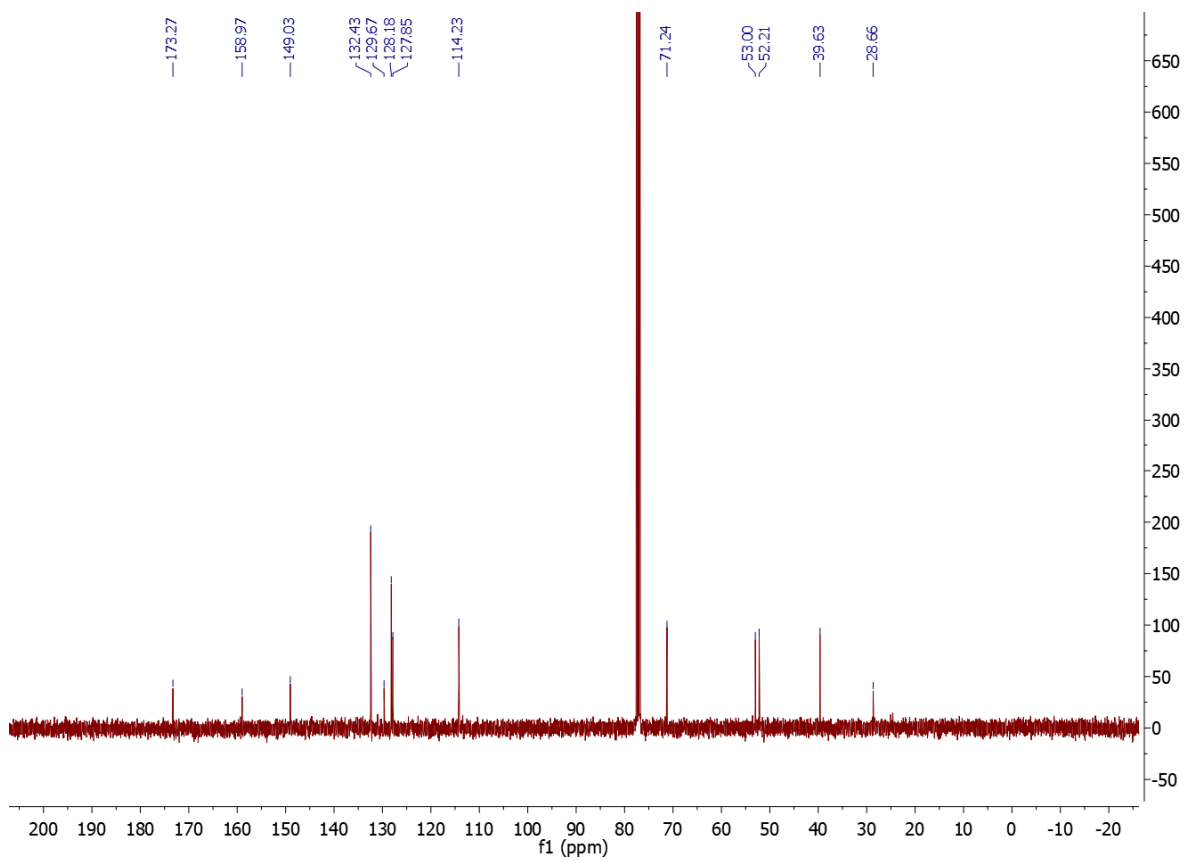
Compound 3ca, ¹H NMR and ¹³C NMR (CDCl₃)
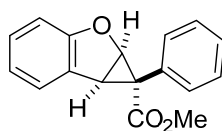
3ca
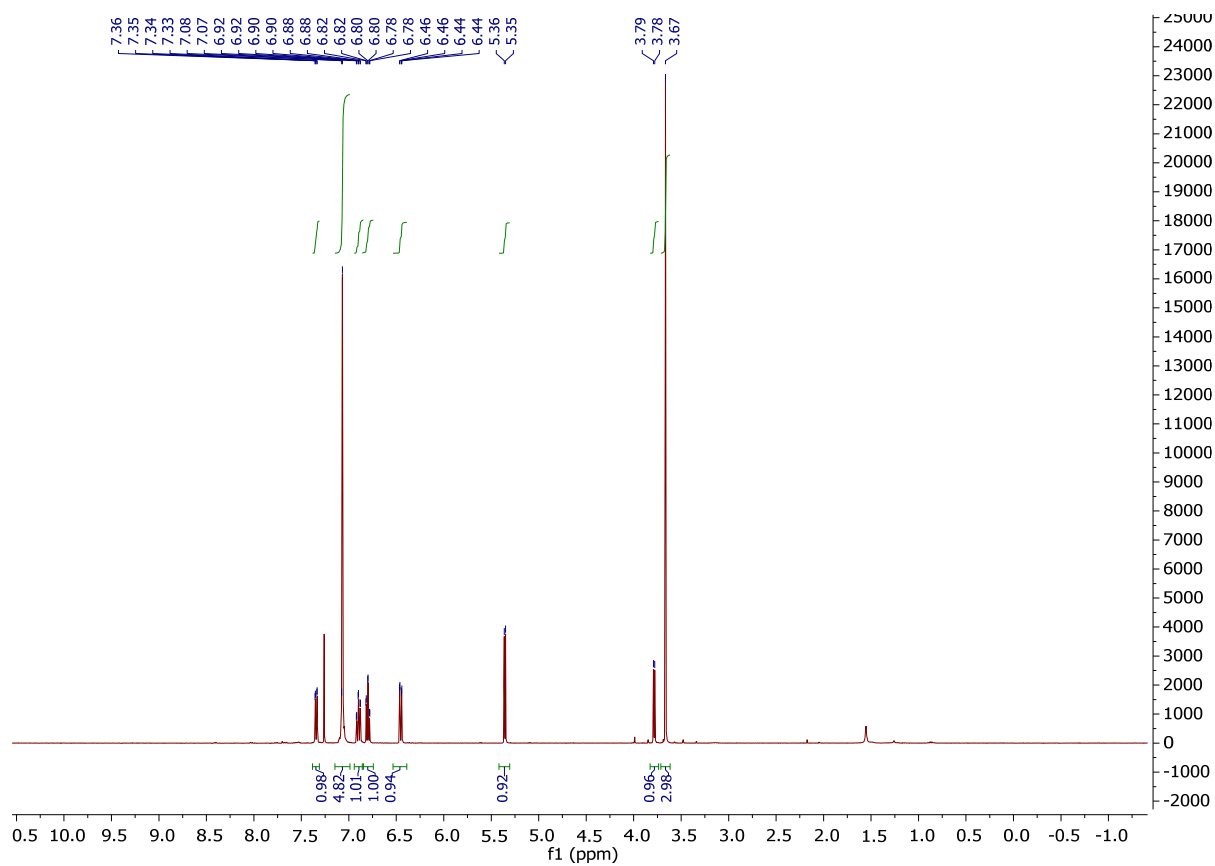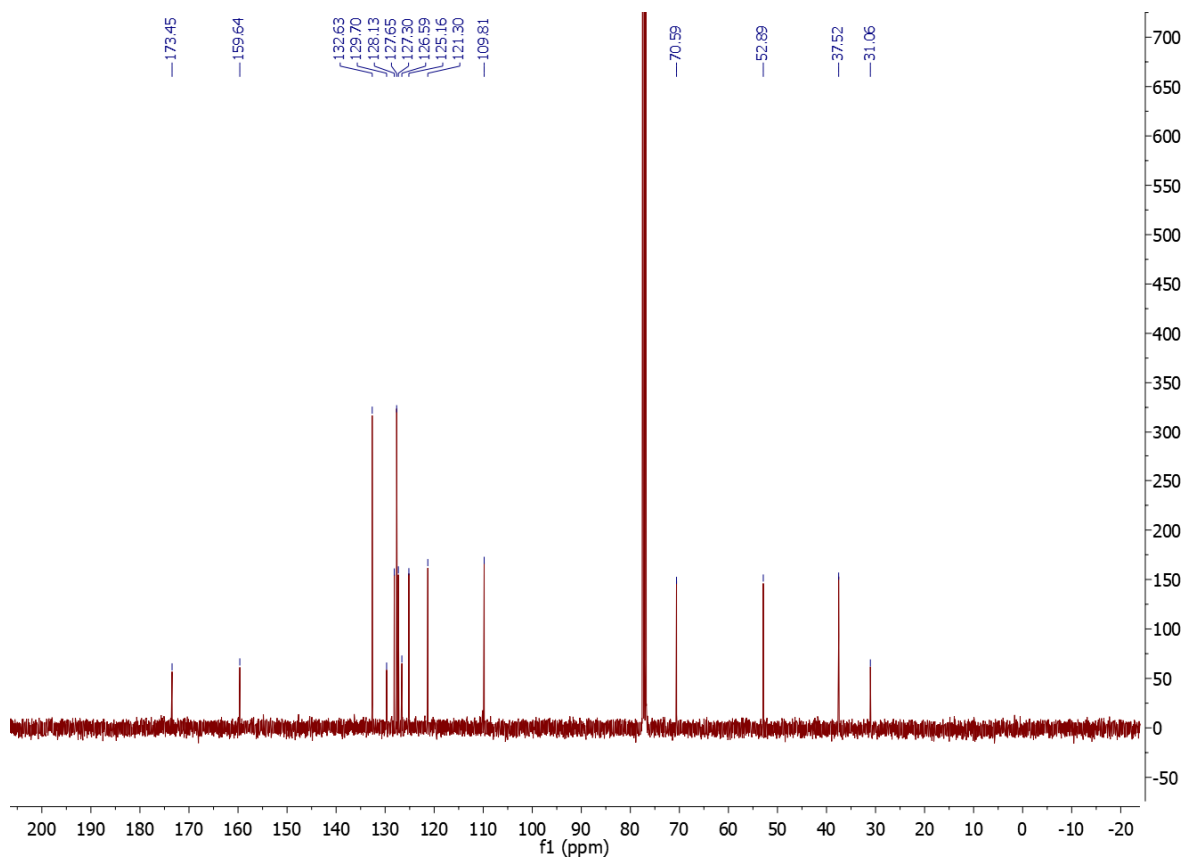
Compound 3da, ¹H NMR and ¹³C NMR (CDCl₃)

3da

43

44
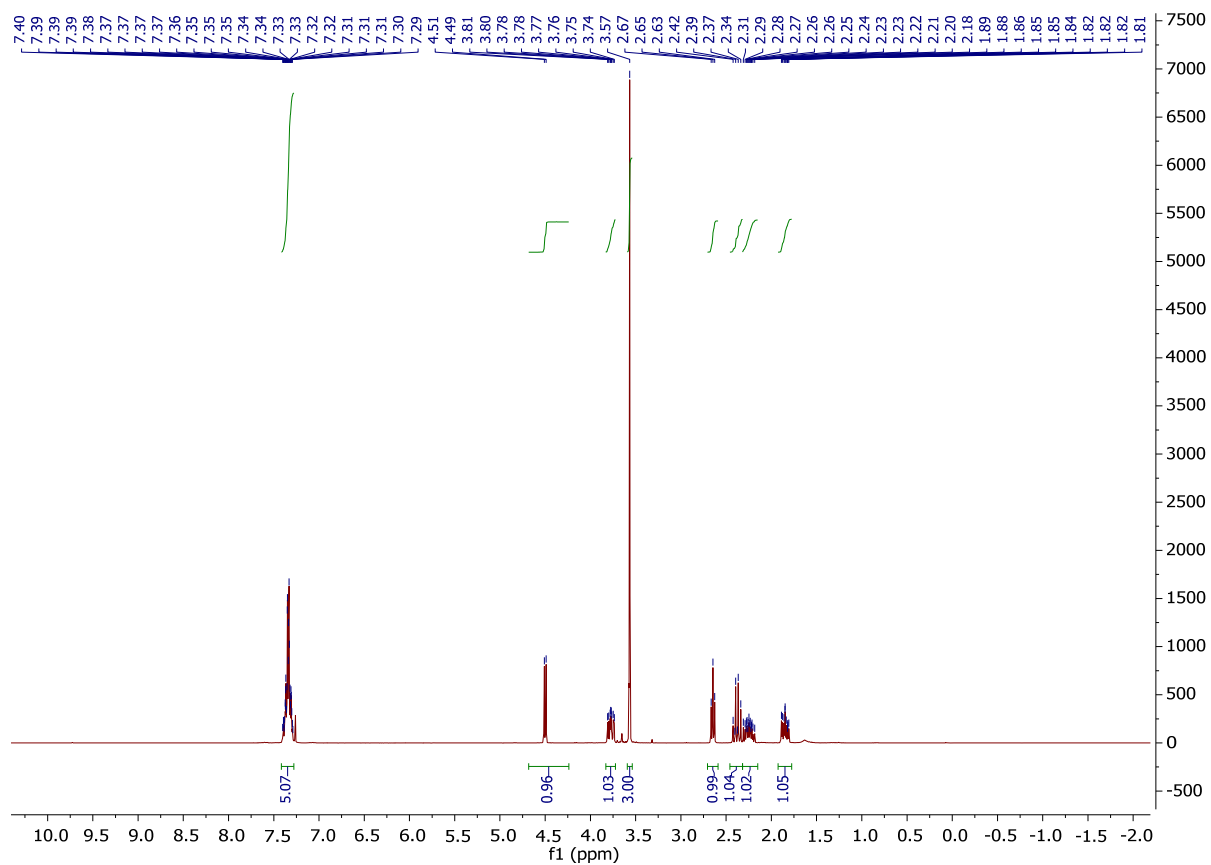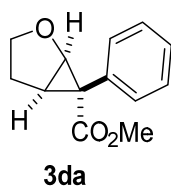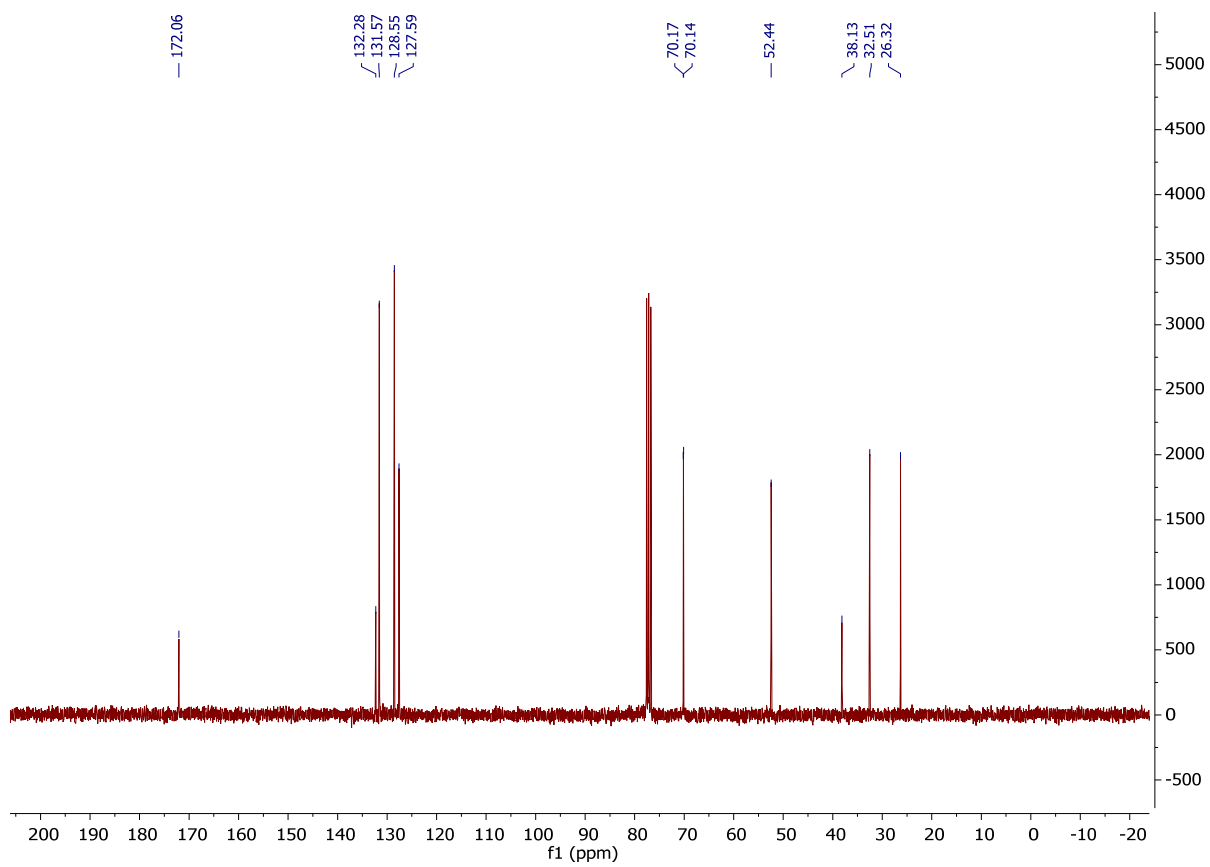
Compound 3ea, ¹H NMR and ¹³C NMR (CDCl₃)
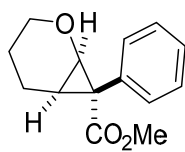
3ea
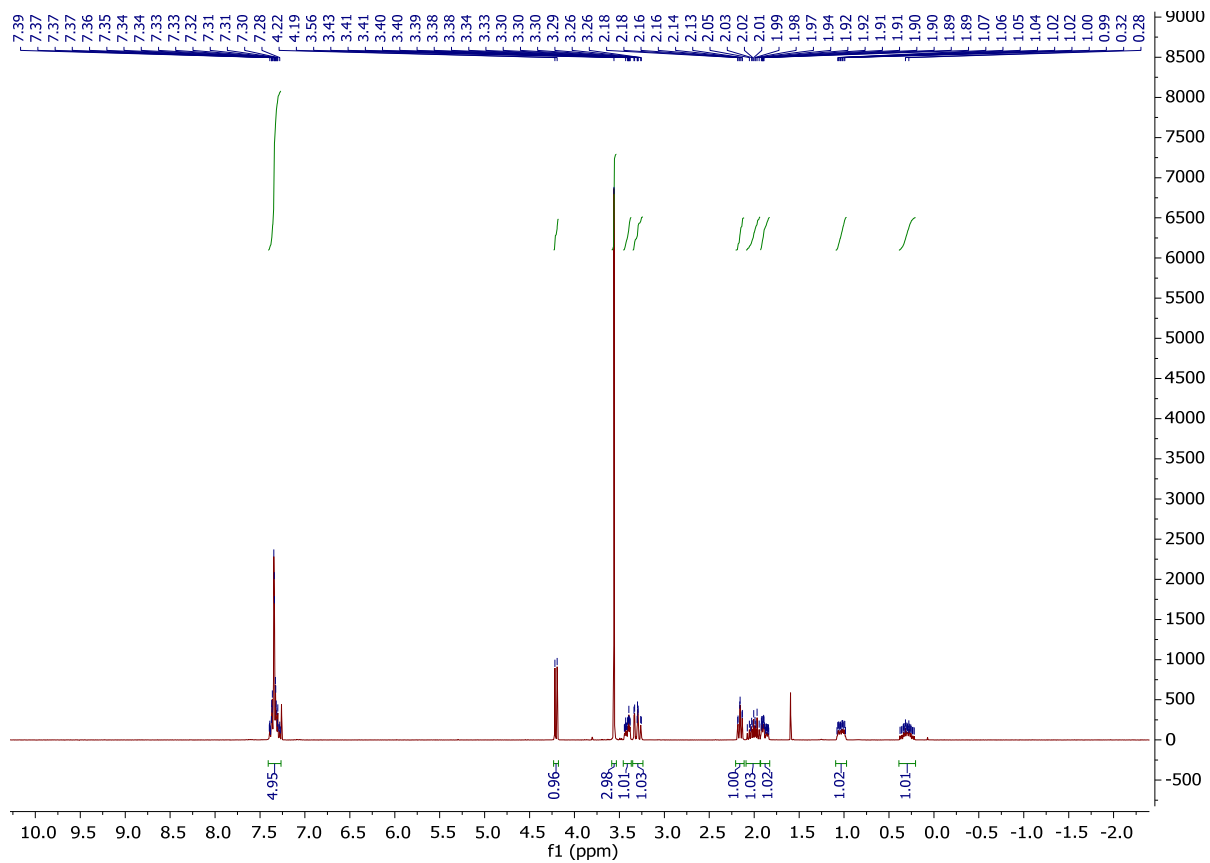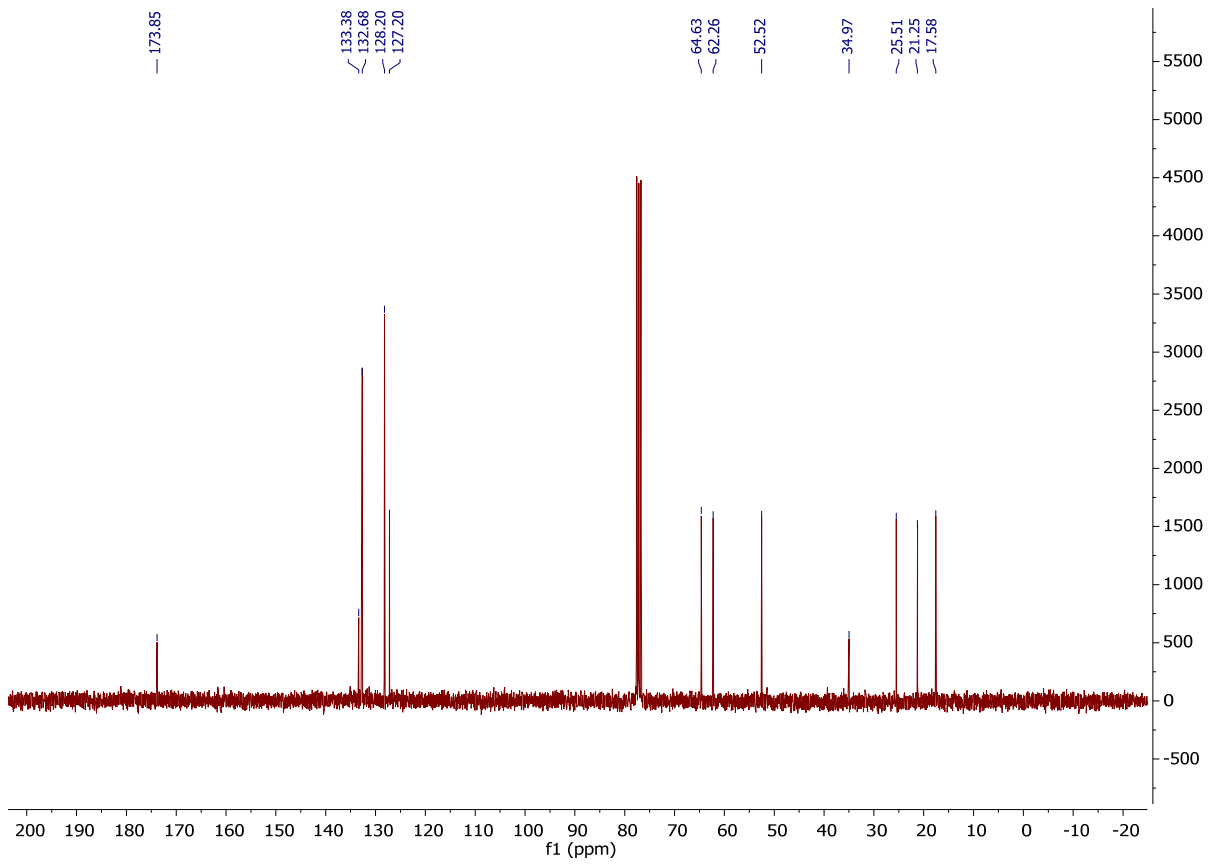
Compound 3fa, ^{1}H NMR and ^{13}C NMR (CDCl$_3$)

3fa

48
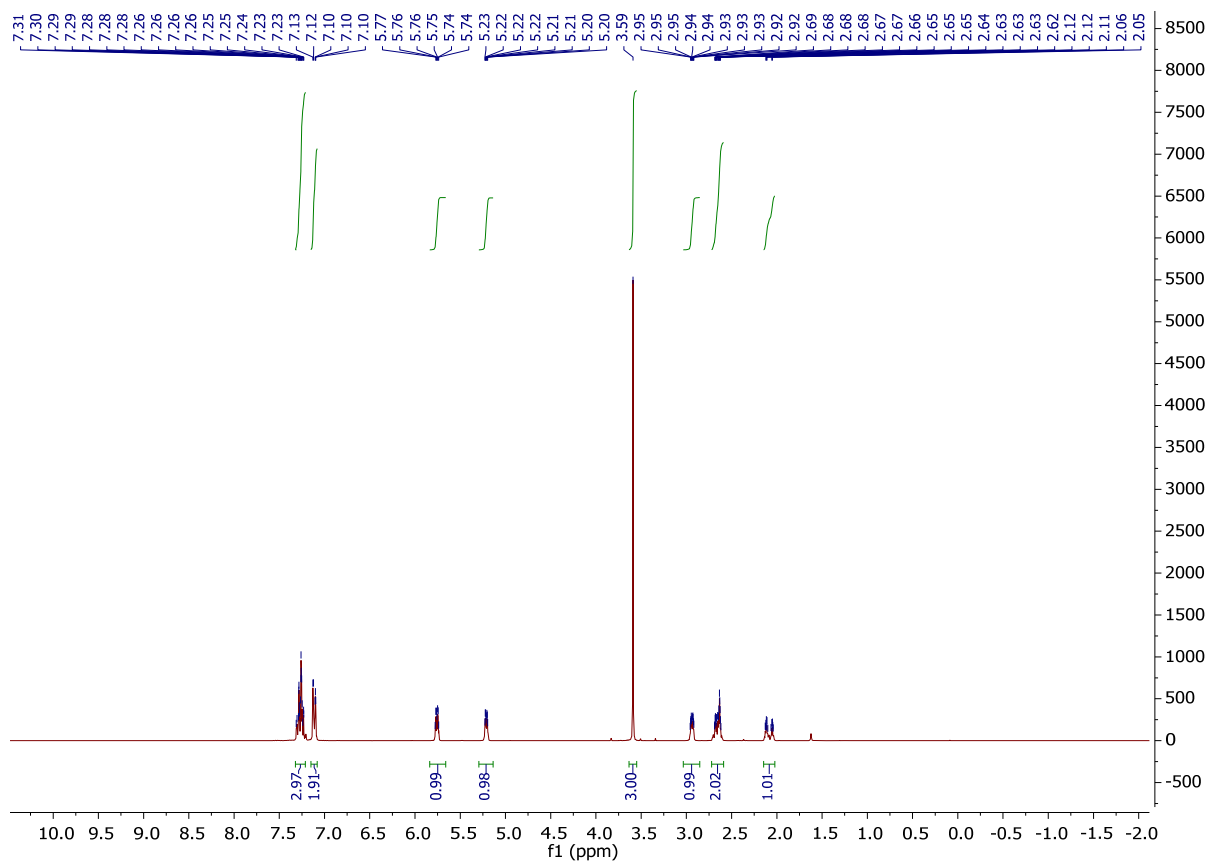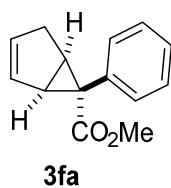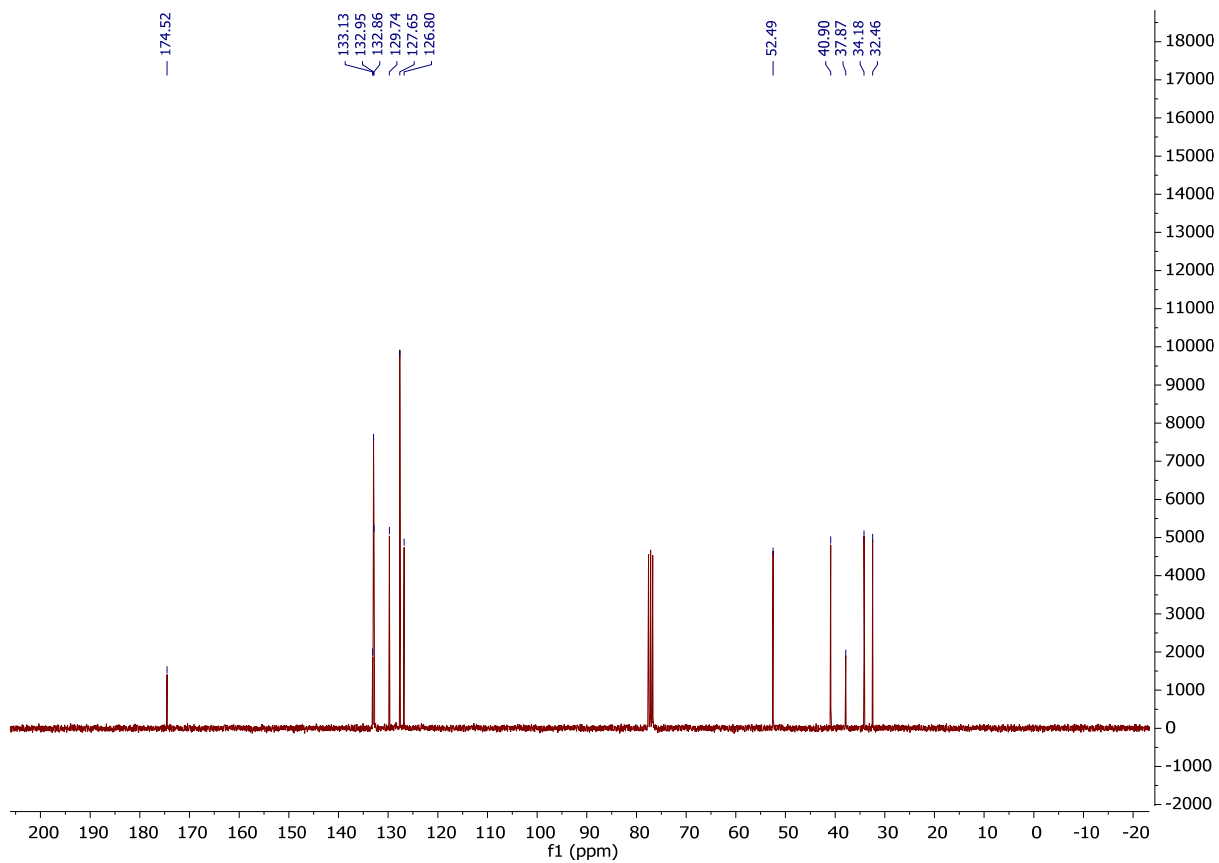
Compound 3ga, ^{1}H NMR and ^{13}C NMR (CDCl$_3$)

3ga

50
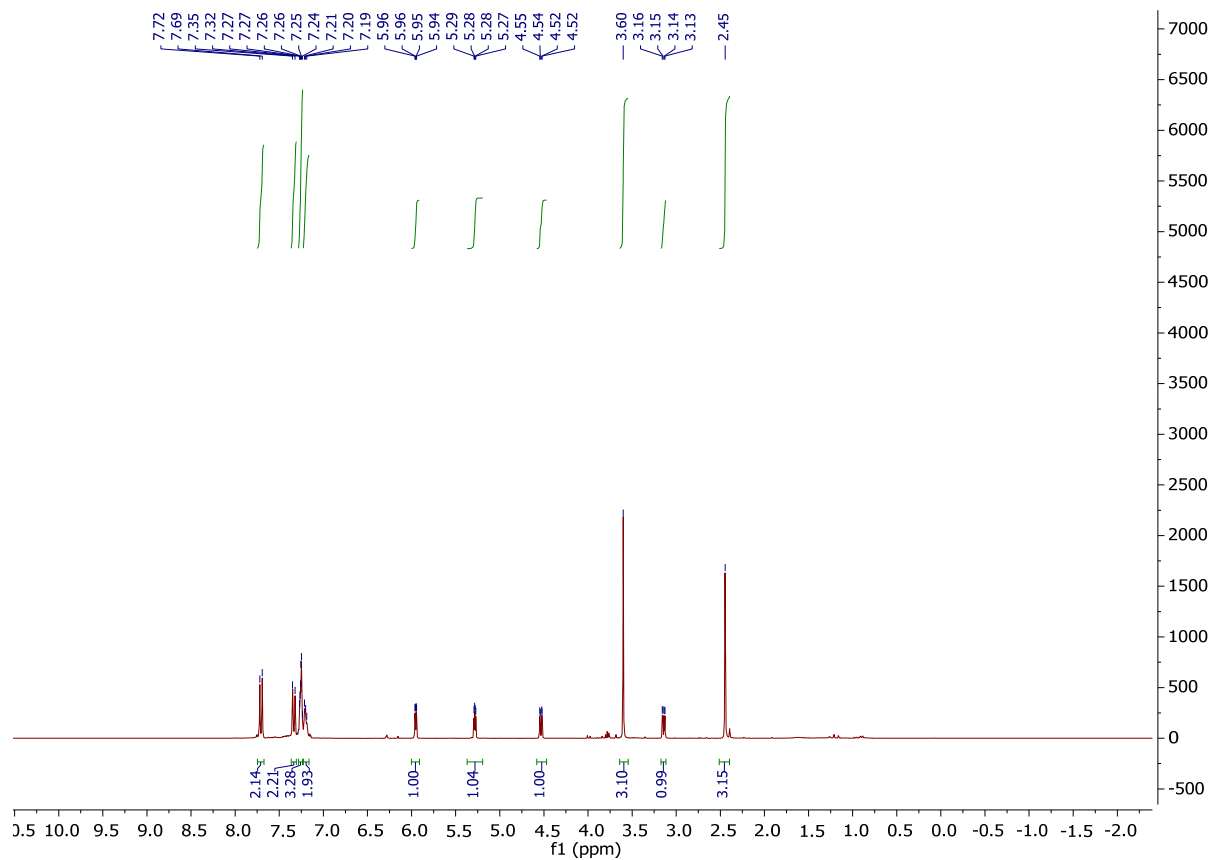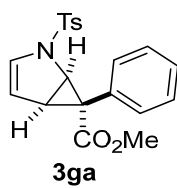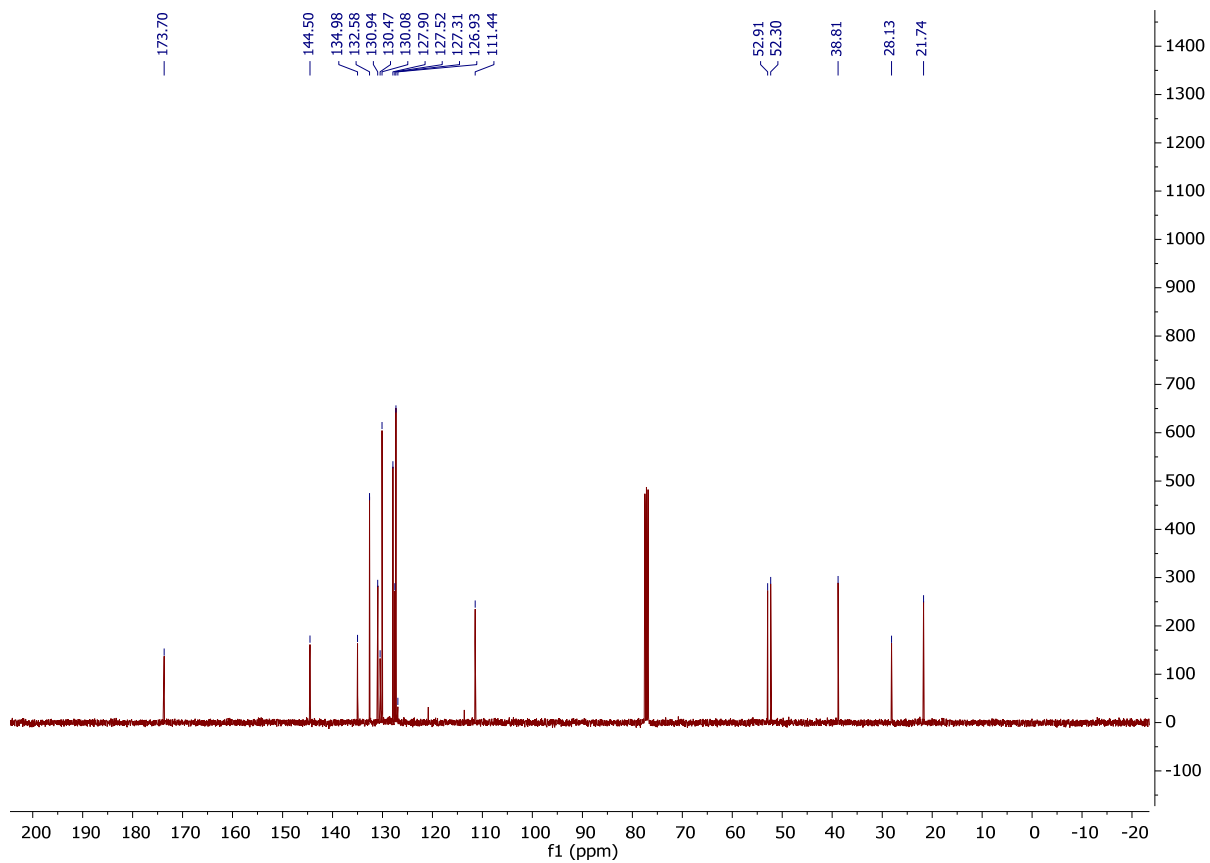
Compound 3ha, ¹H NMR and ¹³C NMR (CDCl₃)

3ha
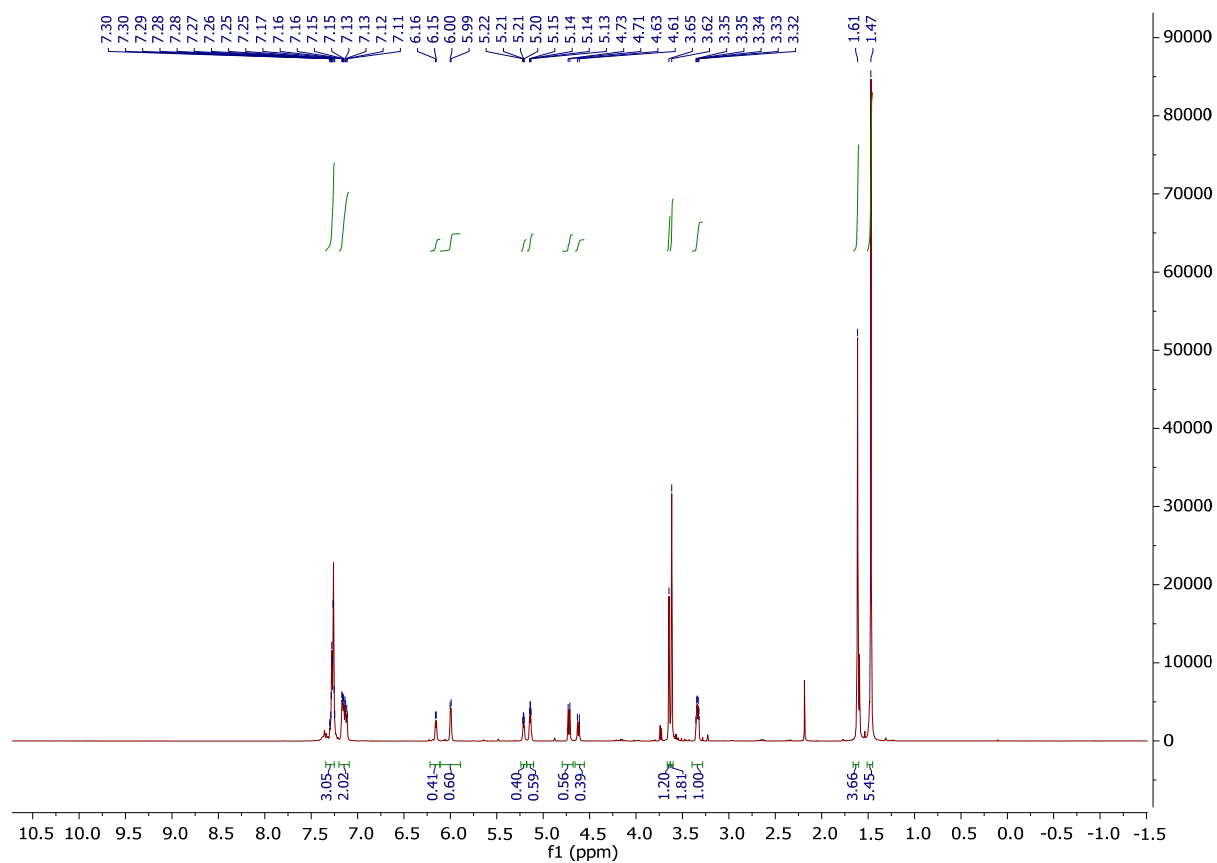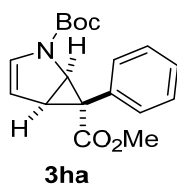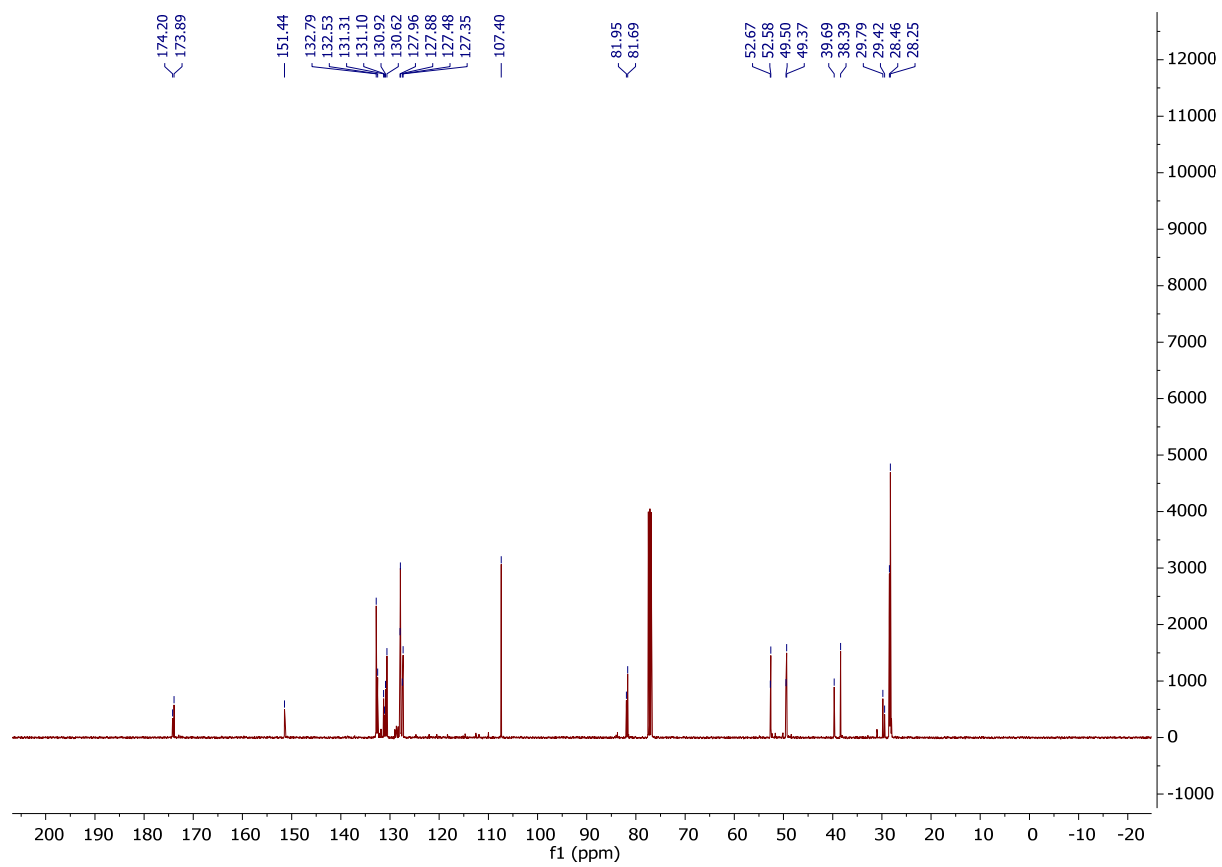
Compound 3ia, ¹H NMR and ¹³C NMR (CDCl₃)

3ia

54
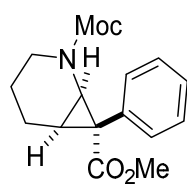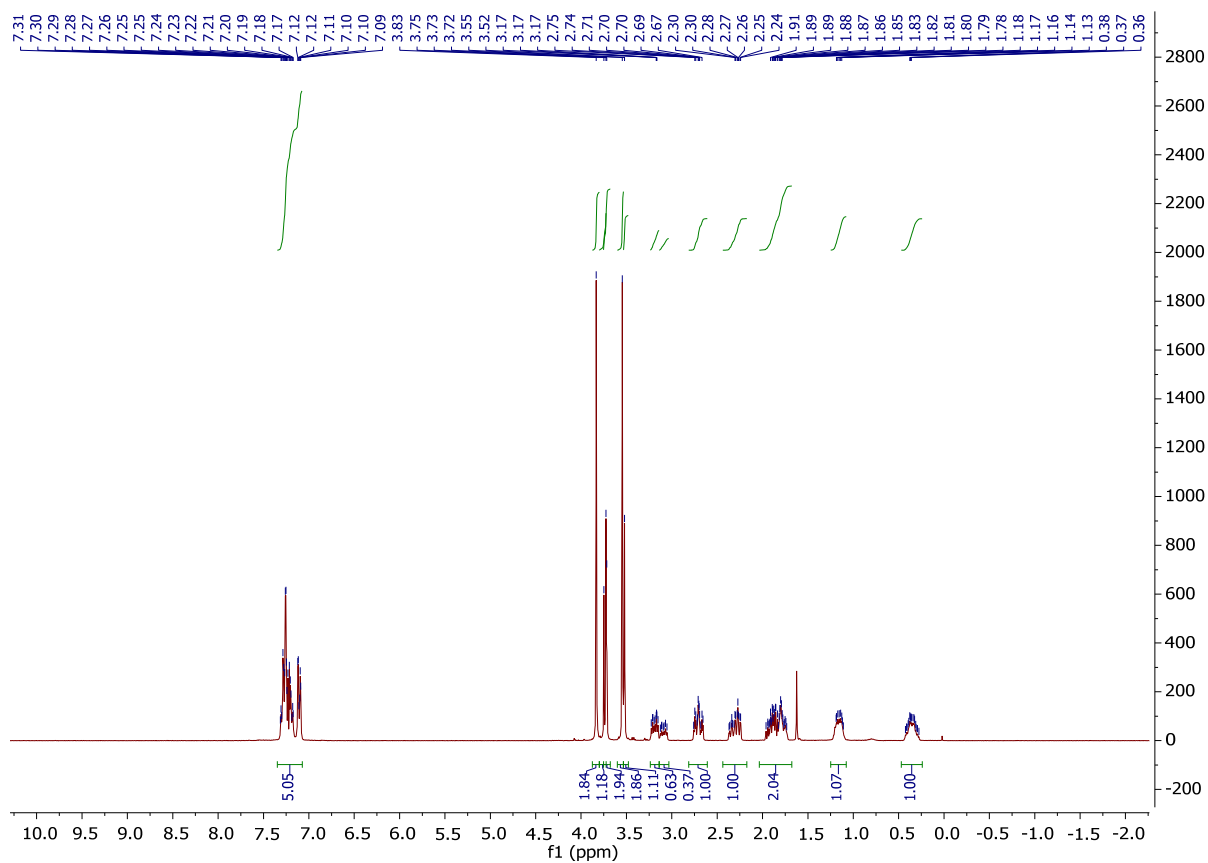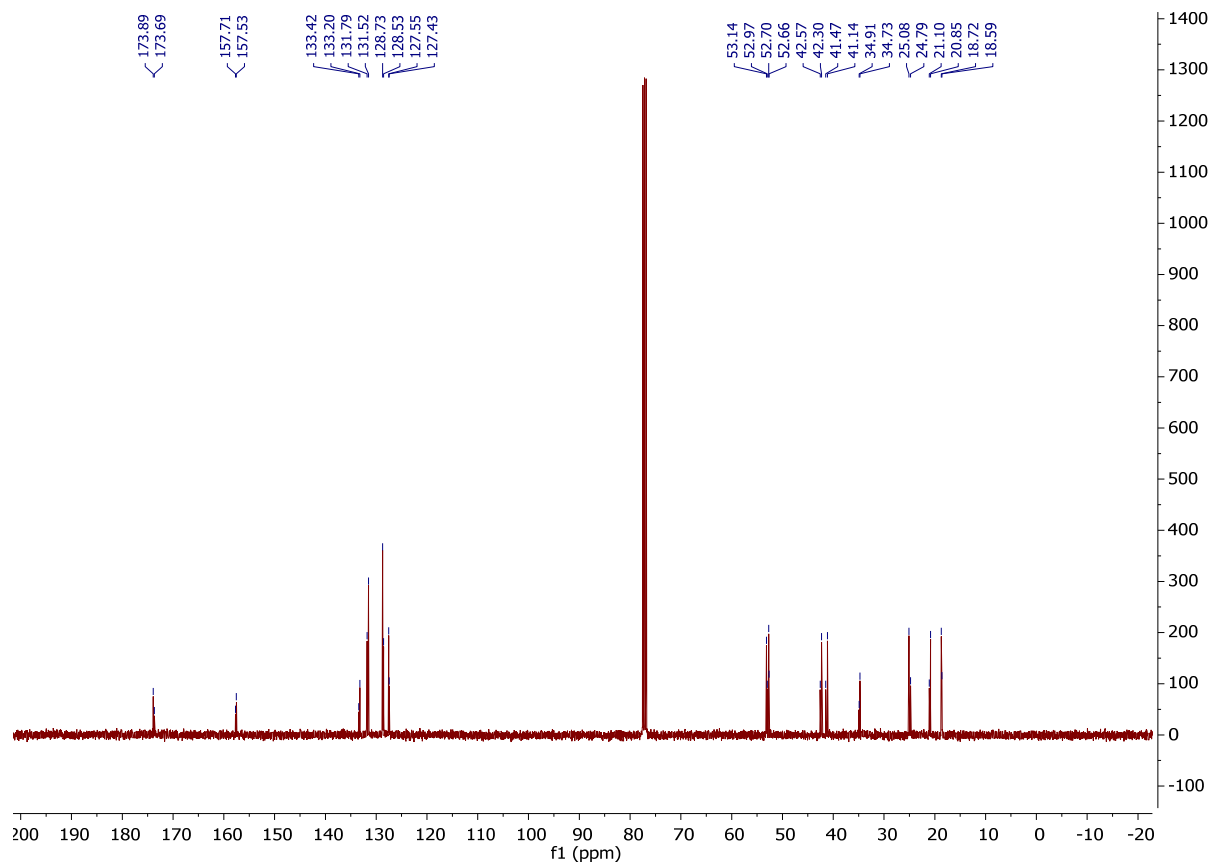
Compound 3ja, ¹H NMR and ¹³C NMR (CDCl₃)

3ja
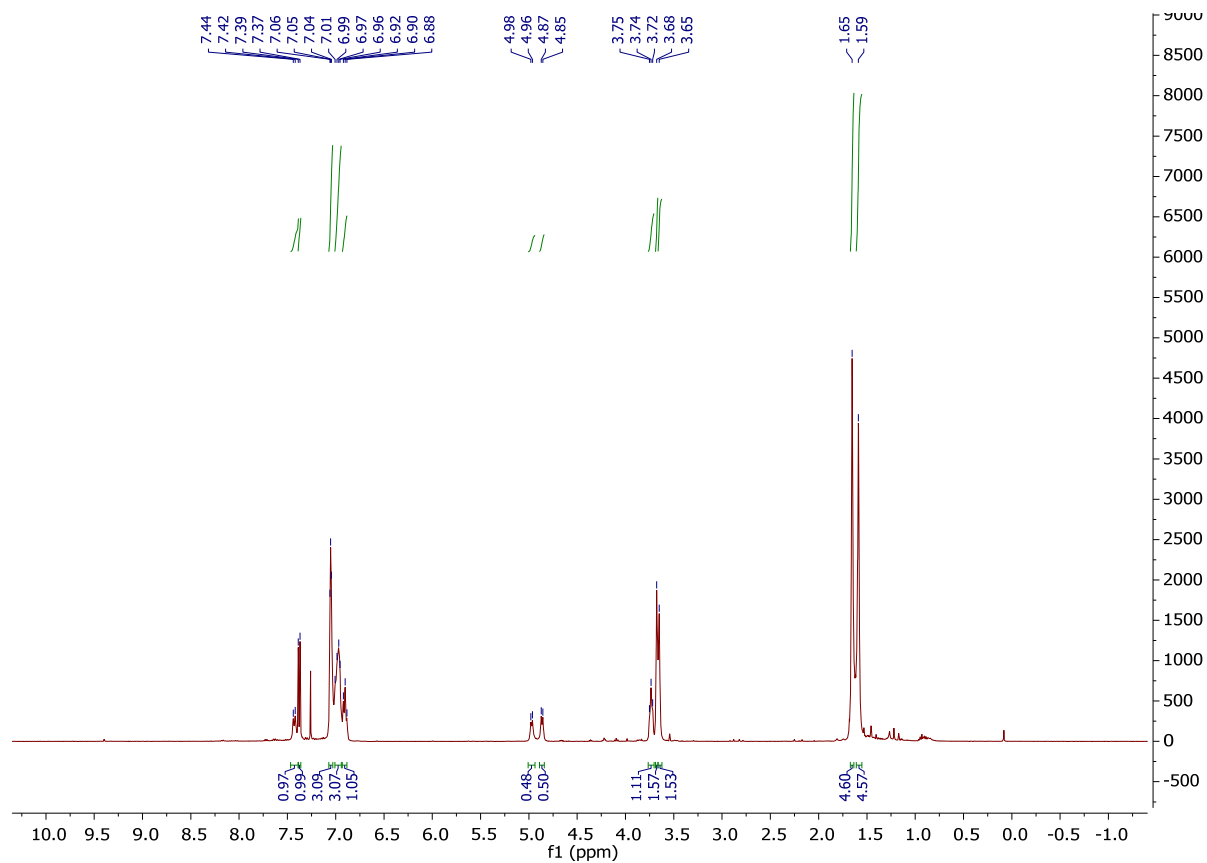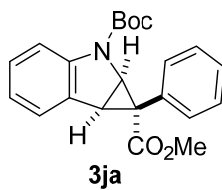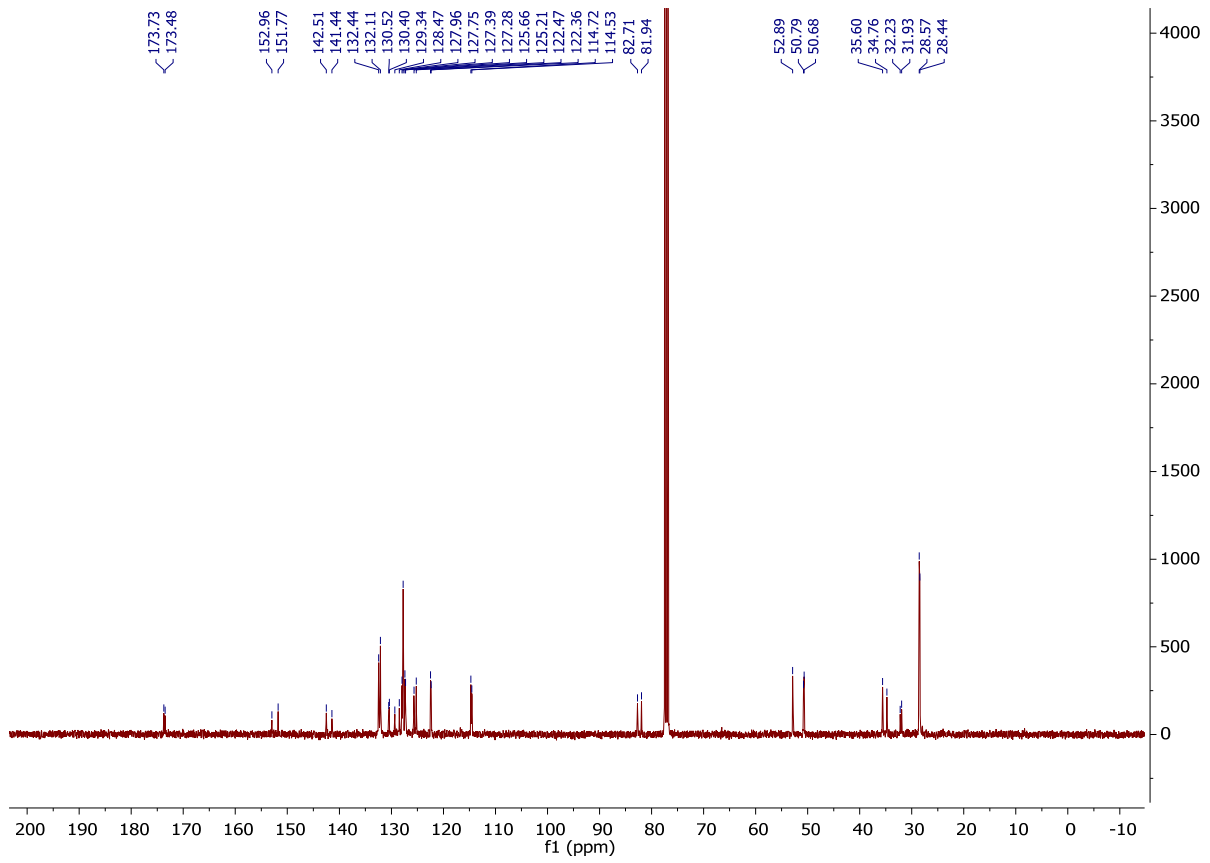
Compound 3fa, ^{1}H NMR, ^{13}C NMR and ^{19}F NMR (CDCl$_3$)

3ka
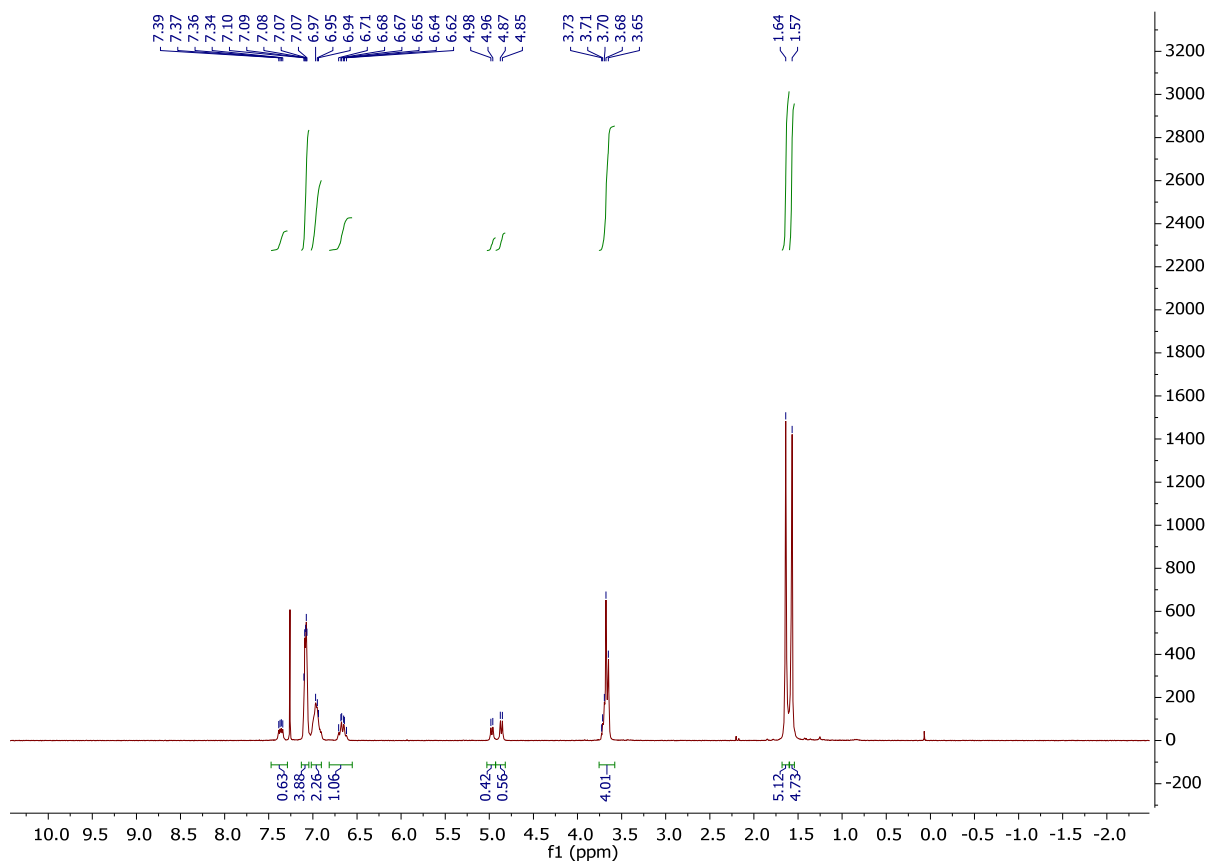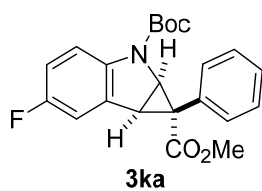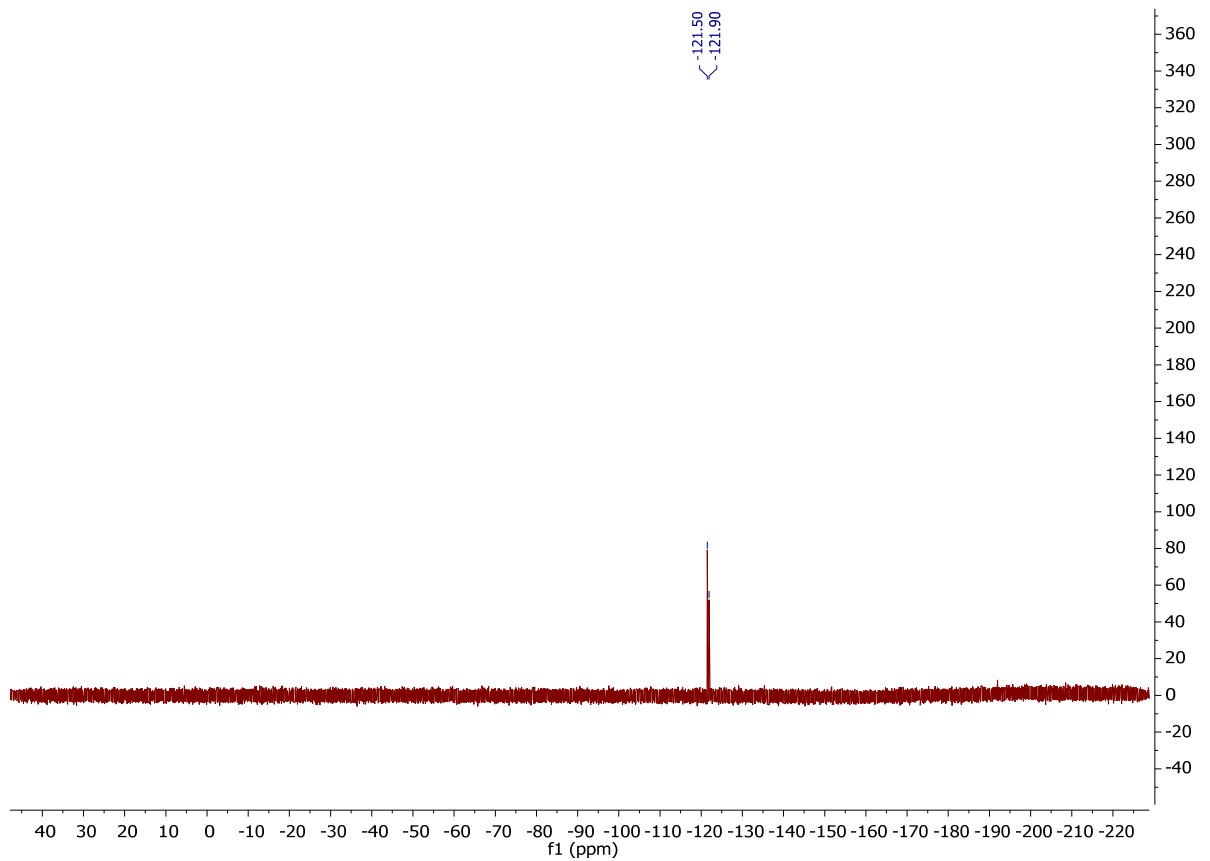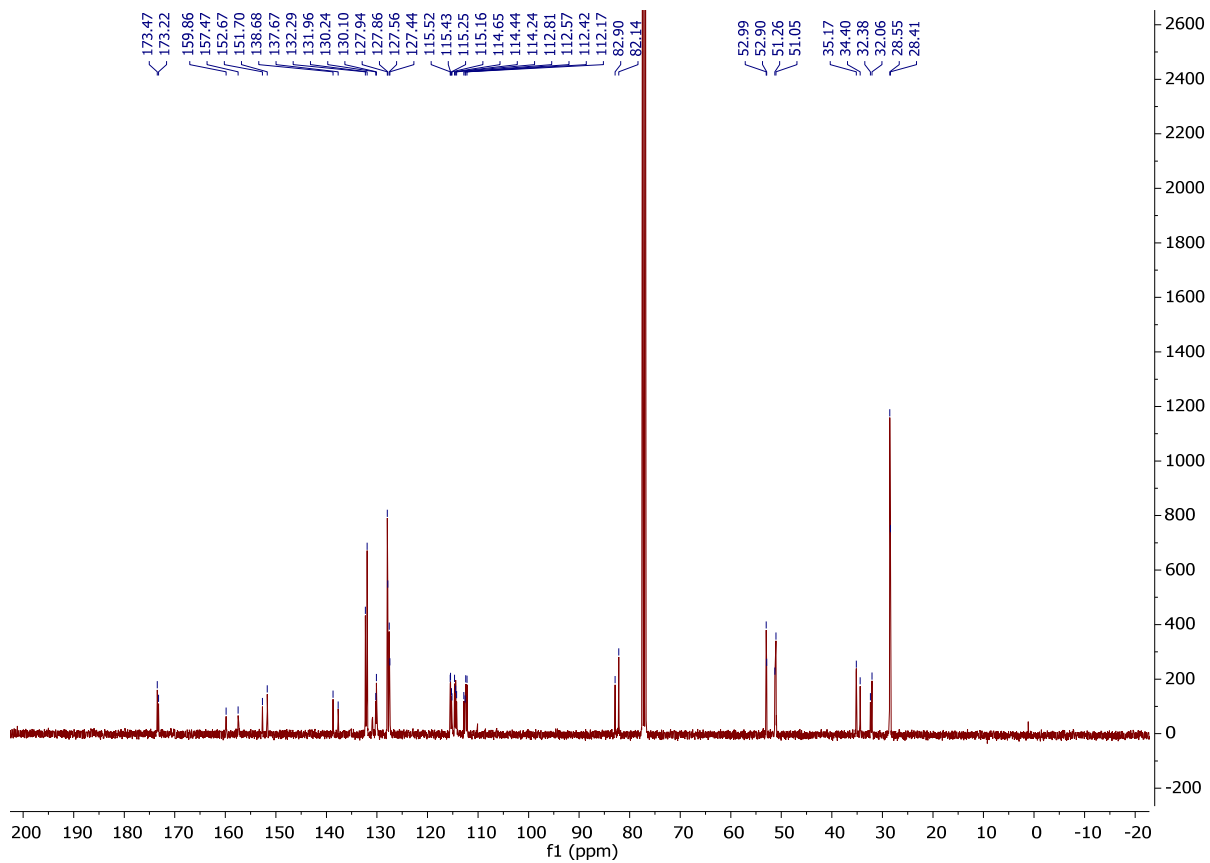
Compound 3la, ^1H NMR and ^{13}C NMR (CDCl$_3$)
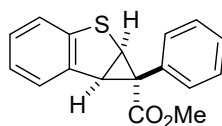
3la
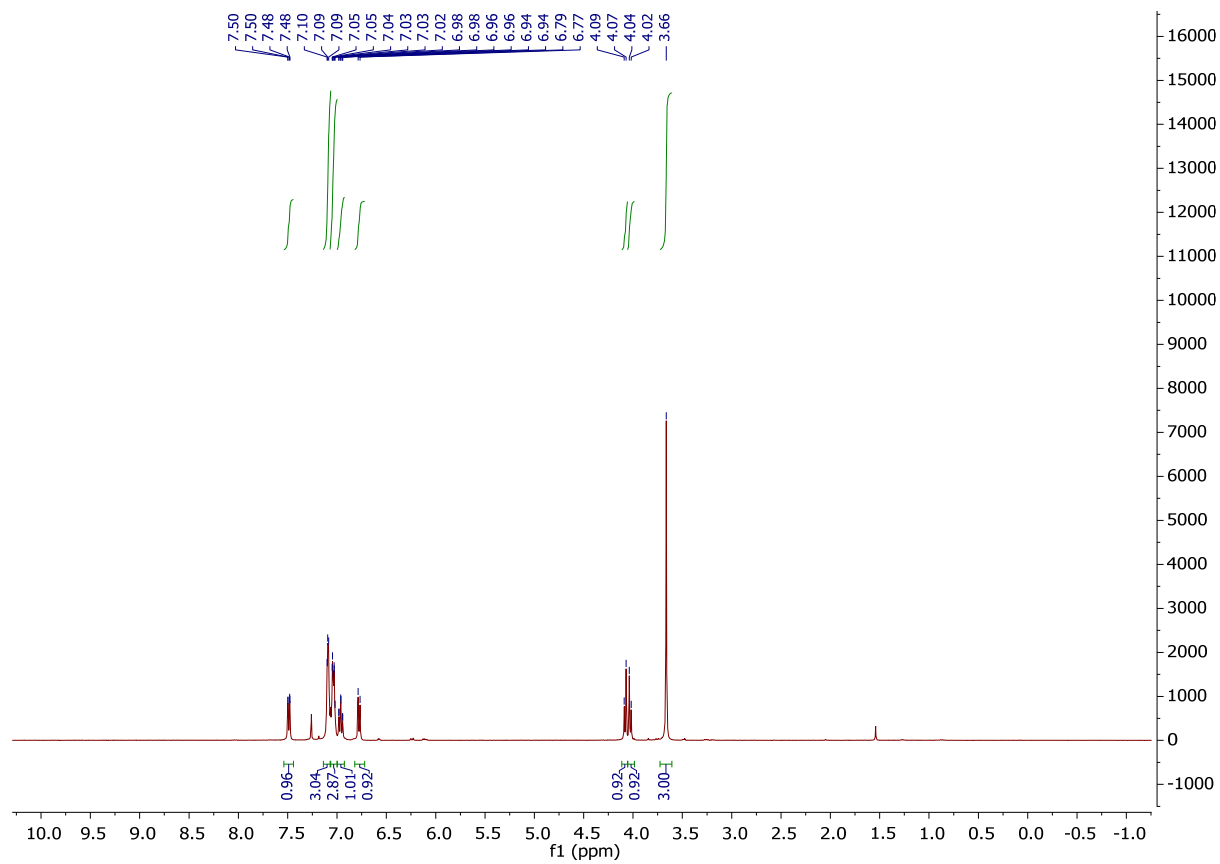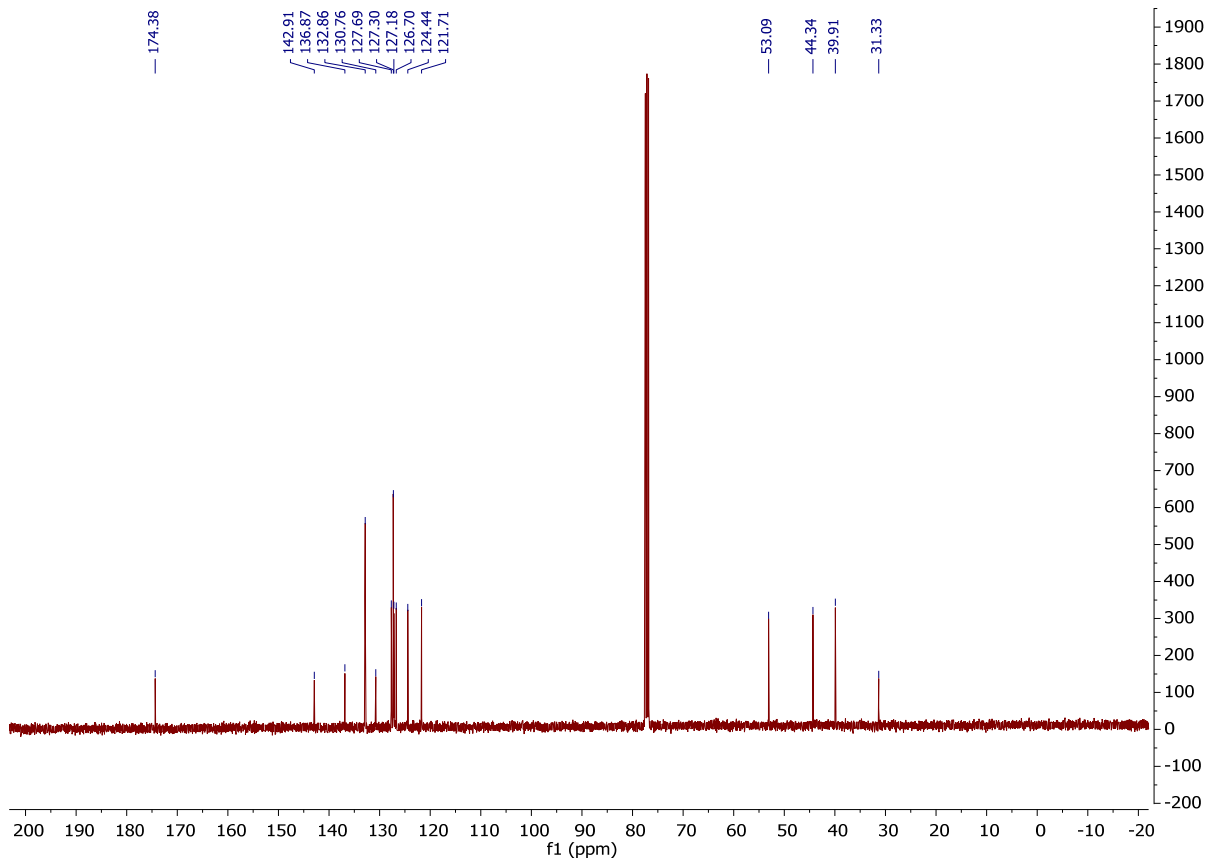
Compound 3ab, ¹H NMR and ¹³C NMR (CDCl₃)

¹H NMR spectrum of compound 3ab in CDCl₃
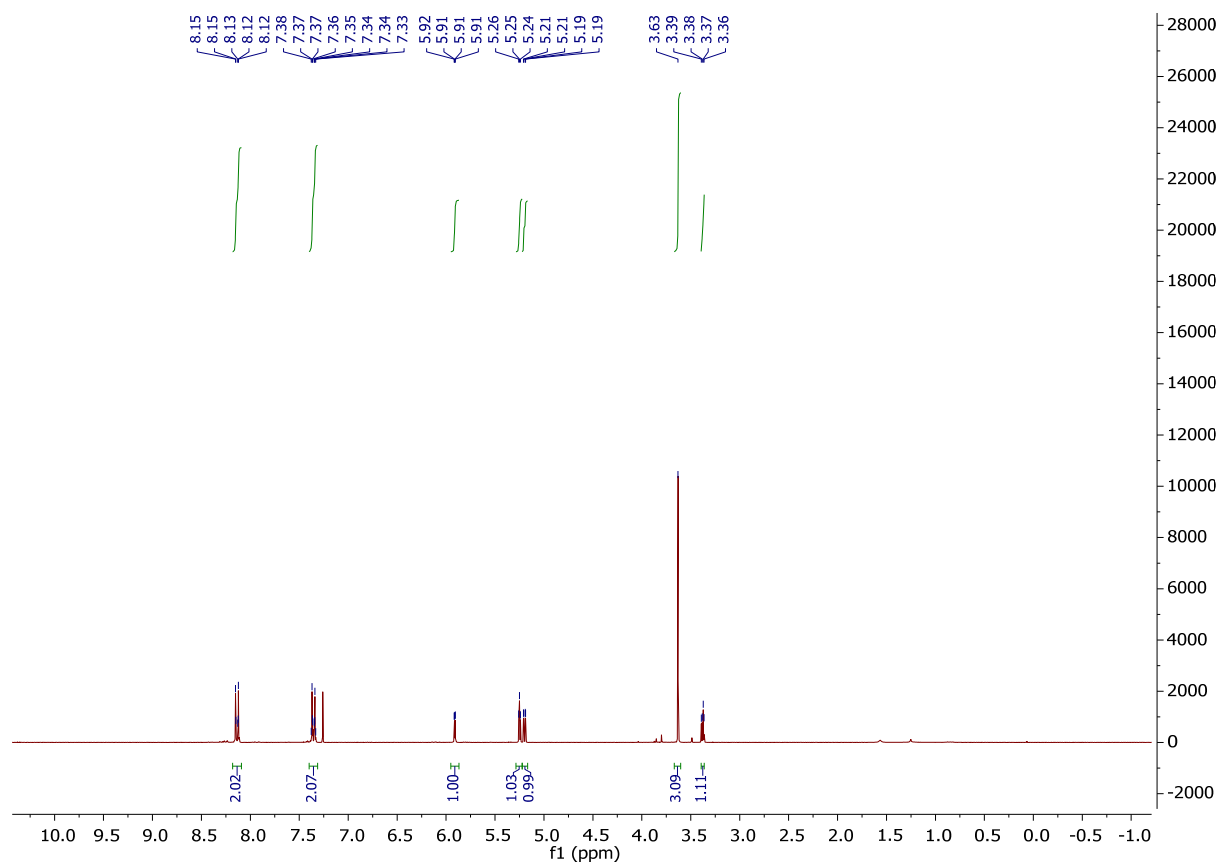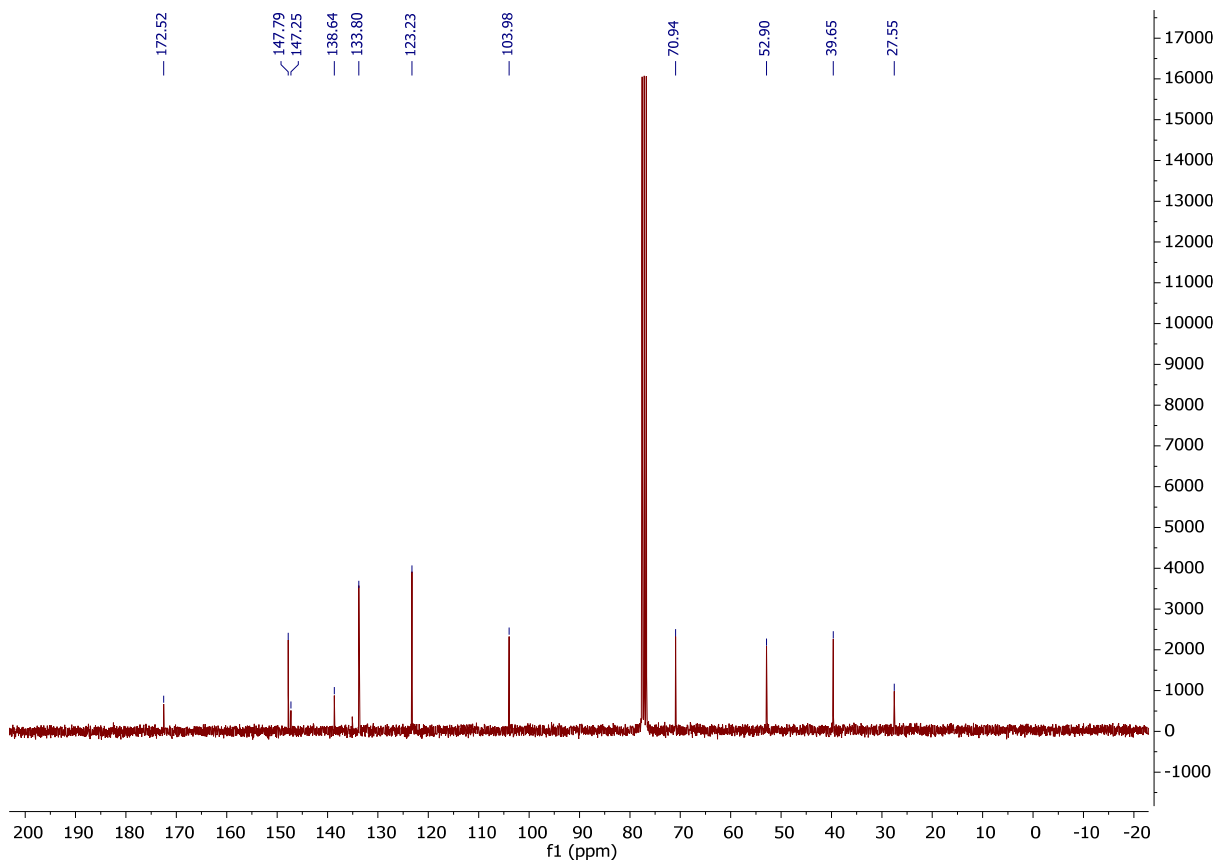
Compound 3ac, ¹H NMR and ¹³C NMR (CDCl₃)

3ac
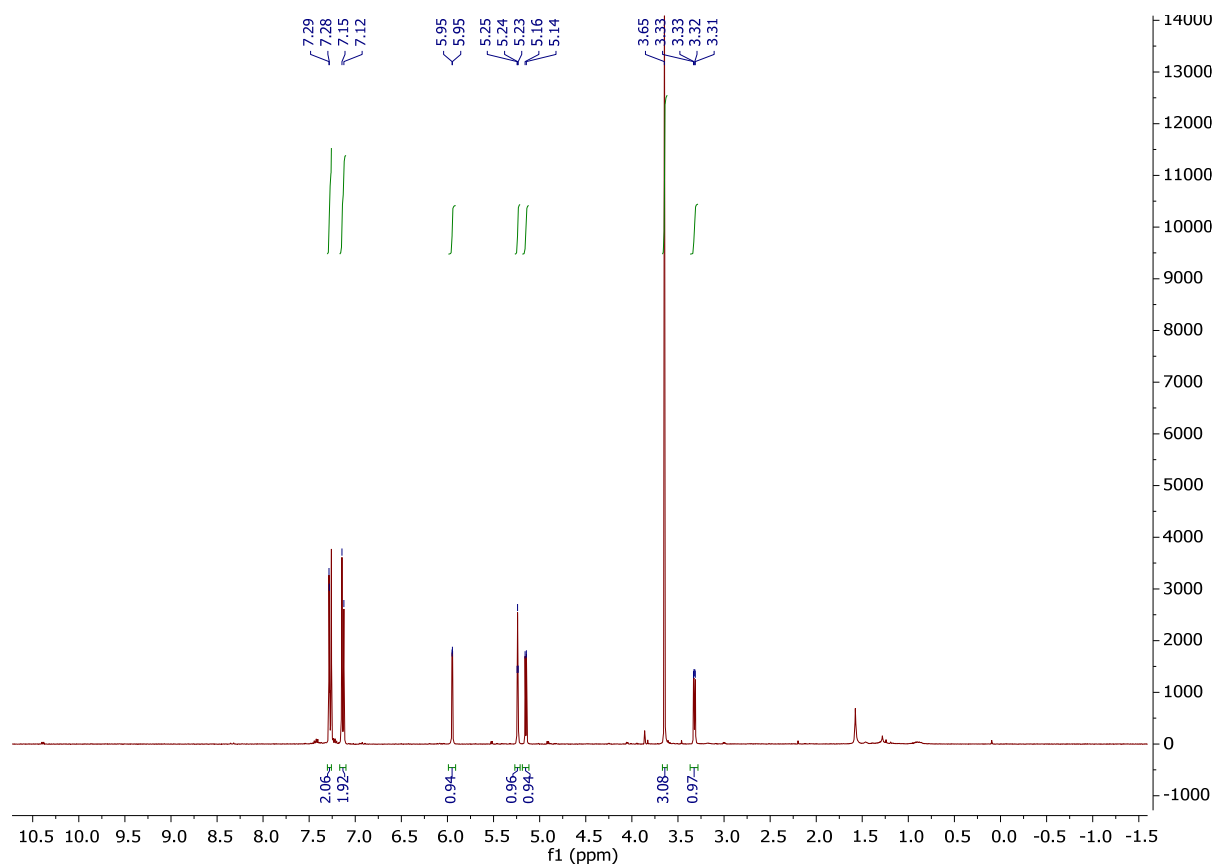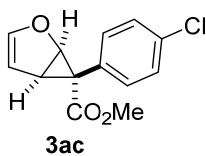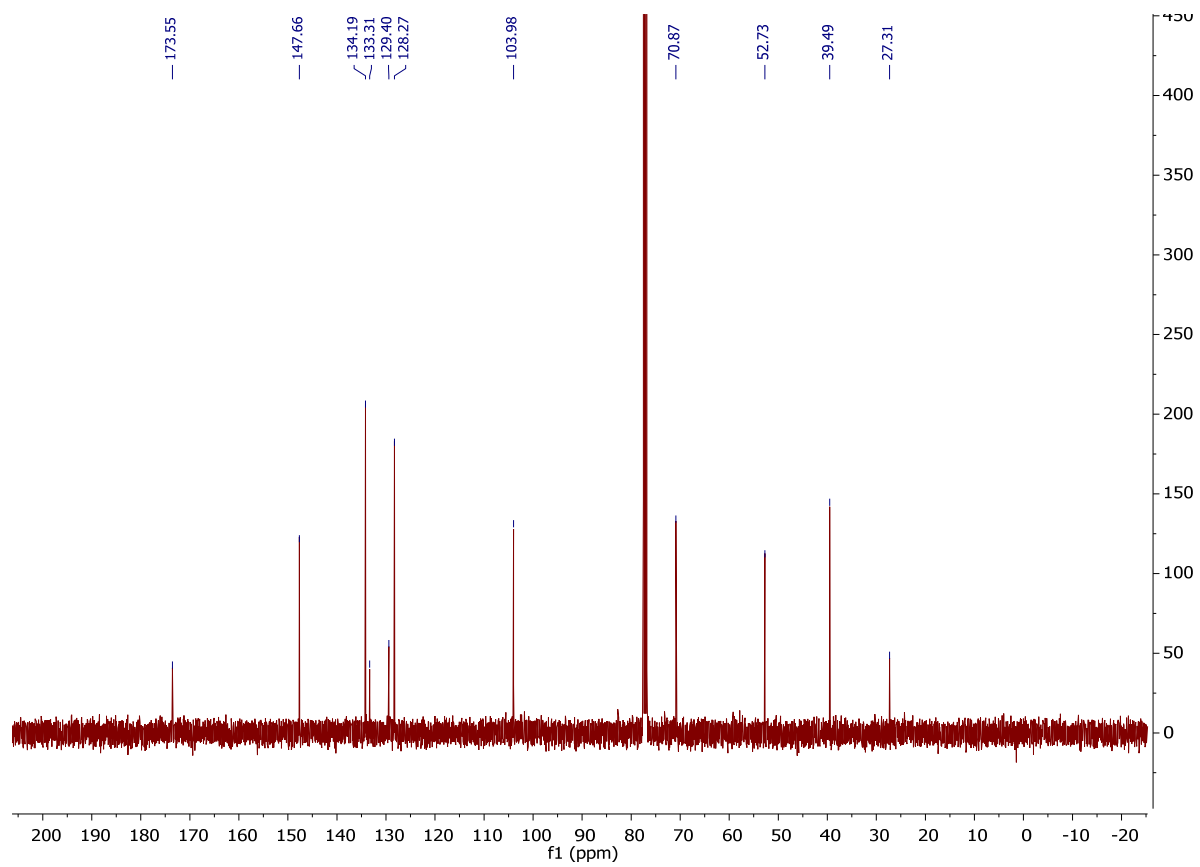
Compound 3ad, ¹H NMR and ¹³C NMR (CDCl₃)

3ad

NMR spectrum with peaks labeled: 174.37, 158.75, 147.51, 133.88, 122.71, 113.42, 104.03, 70.99, 55.23, 52.67, 39.55, 27.24
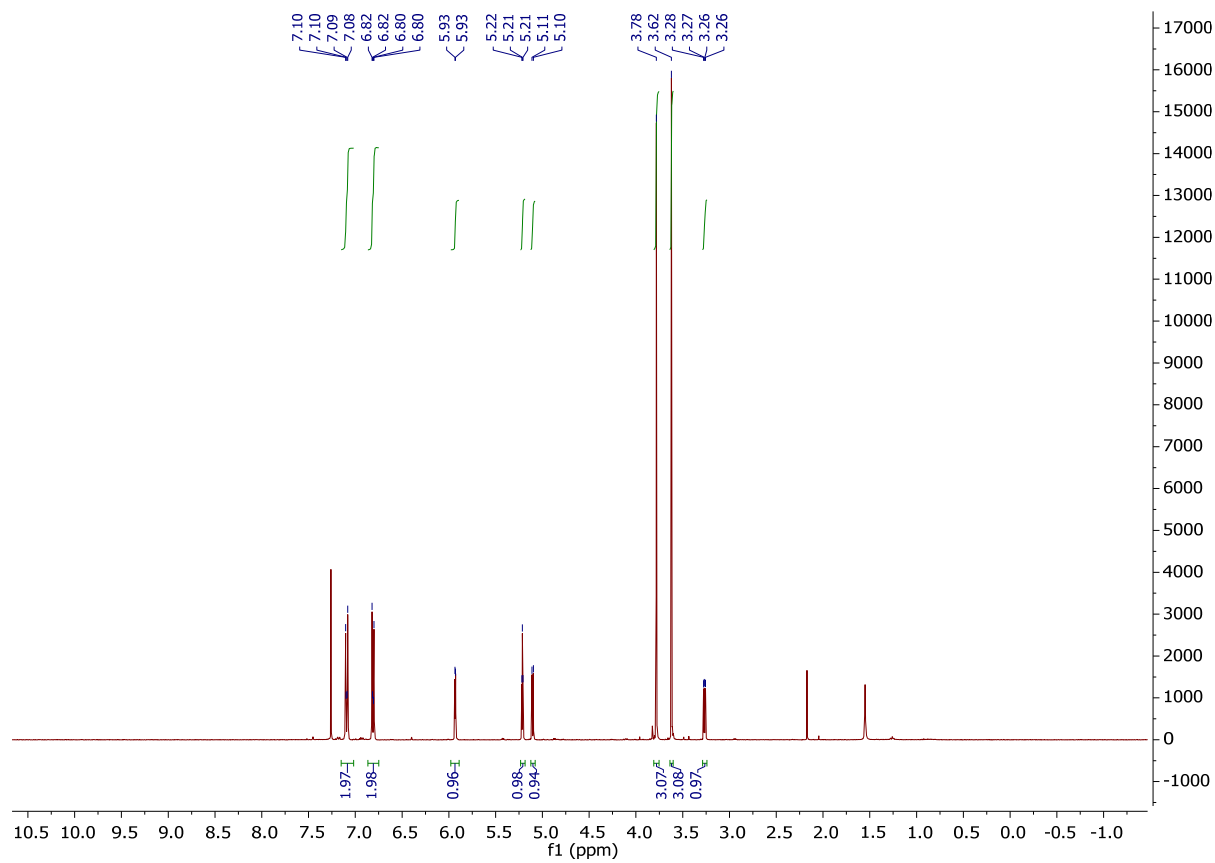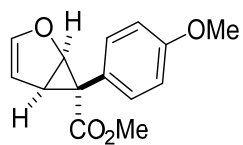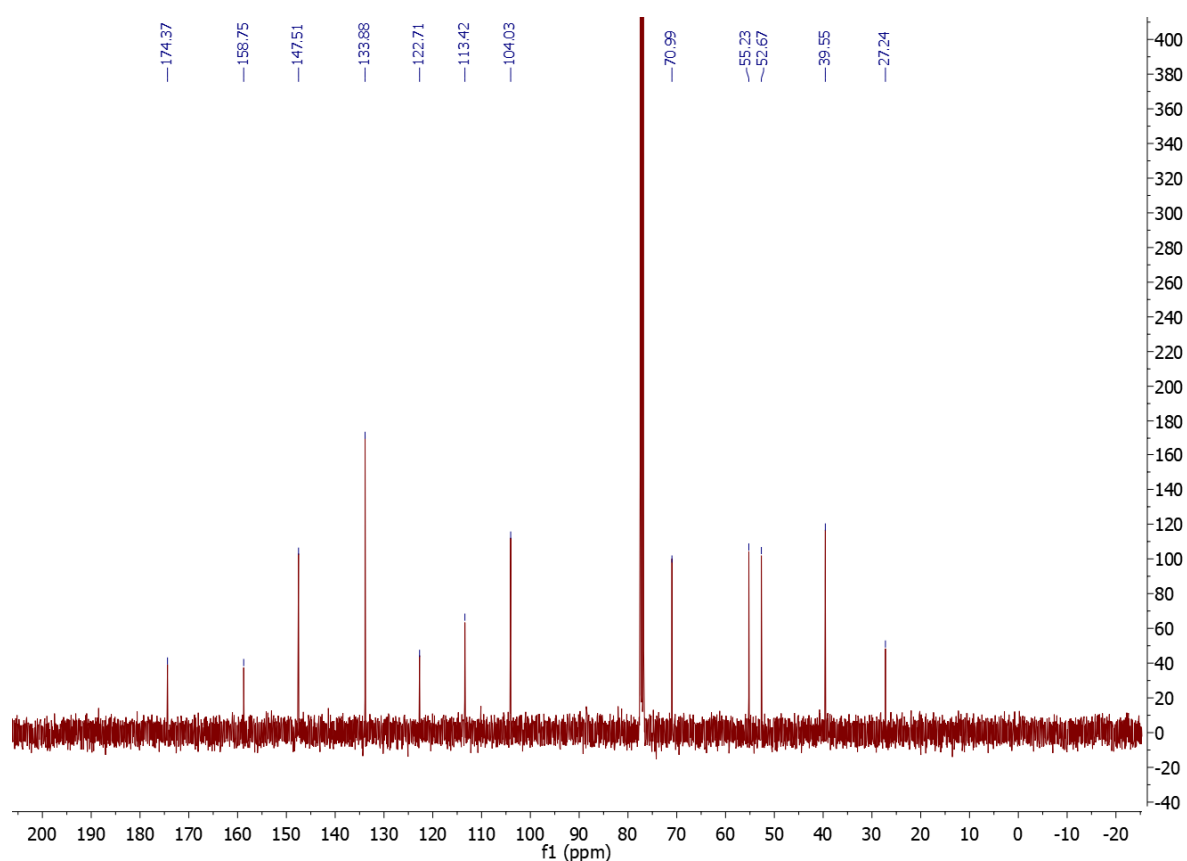
6 X-Ray Crystallography

Single crystal x-ray diffraction data were recorded for a suitable crystal of **3la**. The crystal was mounted on a MITIGEN holder with inert oil on a XtaLAB Synergy R, DW 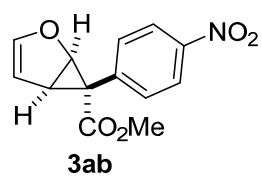system, HyPix-Arc 150 diffractometer using Cu-K_a radiation (λ= 1.54184 Å). The crystal was kept at a steady T = 123.00(10) K during data collection. Empirical multi-scan[12] and analytical absorption corrections[13] were applied to the data. Structures were solved using SHELXT[14] using dual methods and Olex2 as the graphical interface,[15] and least-squares refinements on F^2 were carried out using SHELXL.[14,16]

All non-hydrogen atoms were refined anisotropically. Hydrogen atom positions were calculated geometrically and refined using the riding model. Most hydrogen atom positions were calculated geometrically and refined using the riding model, but some hydrogen atoms were refined freely.

2091948 (**3la**) contain the supplementary crystallographic data for this paper. These data are provided free of charge by The Cambridge Crystallographic Data Centre.

Table S4. Crystallographic data and structure refinement for **3la**.

Compound	3la
Empirical formula	$C_{17}H_{14}O_2S$
ρ_{calc}/(g/cm^3)	1.376
μ/mm^{-1}	2.089
Formula weight	282.34 g mol^{-1}
Crystal colour	clear colourless
Crystal shape	block-shaped
Crystal size/mm^3	0.14 × 0.13 × 0.11
Temperature/K	123.00(10)
Crystal system	monoclinic
Space group	$P2_1/c$
a/Å	11.6106(3)
b/Å	16.0508(3)
c/Å	7.5624(2)
α/°	90
β/°	104.790(2)
γ/°	90
Volume/Å^3	1362.63(6)
Z	4
Z'	1
Wavelength/ Å	1.54184
Radiation	Cu K$_\alpha$
Θ_{min}/°	3.938
Θ_{max}/°	73.823
Reflections collected	15601
Independent reflections	2655

Reflections I≥2 σ(I)	2453
R_{int}	0.0250
Parameters	182
Restraints	0
Largest peak	0.614
Deepest hole	-0.677
GooF	1.077
wR_2 (all data)	0.1274
wR_2	0.1254
R_1 (all data)	0.0489
R_1	0.0461
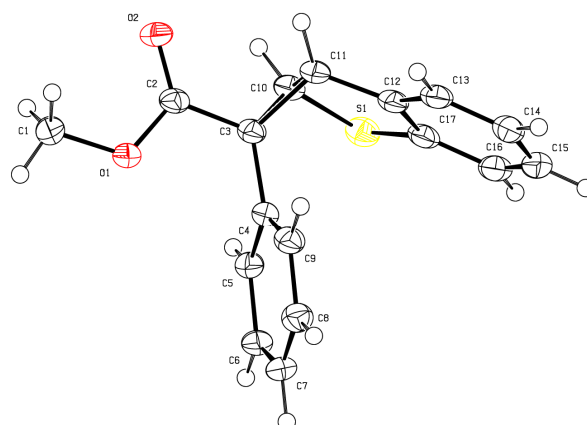
Figure S9. Solid-state molecular structure of **3la**, including atom numbering scheme. Thermal ellipsoids are set at the 50% probability level. C atoms shown in grey, S atom in yellow and O atoms in red.
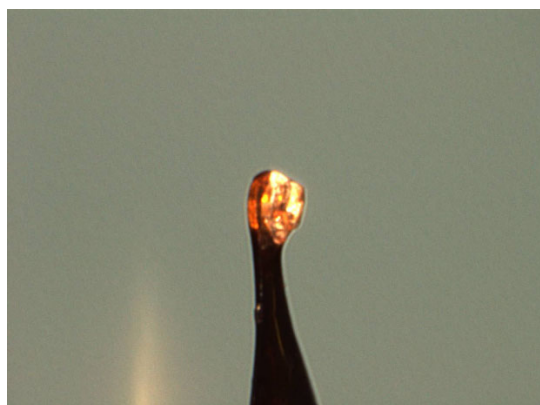
Figure S10. Picture of **3la** crystal inside the diffractometer.

Table S5. Bond lengths for **3la**.

Atom	Atom	Length/Å
S1	C17	1.773(2)
S1	C10	1.782(2)
O1	C2	1.336(2)
O1	C1	1.455 (2)
O2	C2	1.212(2)
C4	C3	1.495(3)
C4	C5	1.391 (3)
C4	C9	1.396(3)
C3	C2	1.496(3)
C3	C11	1.547 (3)
C3	C10	1.540(3)
C12	C11	1.481(3)
C12	C13	1.408(3)
C12	C17	1.399(3)
C5	C6	1.392(3)
C6	C7	1.390(3)
C11	C10	1.503(3)
C13	C14	1.389(3)
C7	C8	1.384(3)
C9	C8	1.391(3)
C17	C16	1.383(3)
C15	C14	1.398(3)
C15	C16	1.366(3)

Table S6. Bond angles for **3la**.

Atom	Atom	Atom	Angle/°
C17	S1	C10	92.01(10)
C2	O1	C1	115.66(15)
C5	C4	C3	120.07(18)
C5	C4	C9	119.13(18)
C9	C4	C3	120.68(18)
C4	C3	C2	117.61(17)
C4	C3	C11	121.08(17)
C4	C3	C10	121.69(17)
C2	C3	C11	112.82(16)
C2	C3	C10	111.87(16)
C10	C3	C11	58.25(13)
C13	C12	C11	126.33(19)
C17	C12	C11	113.73(18)
C17	C12	C13	119.94(19)
O1	C2	C3	112.22(16)
O2	C2	O1	123.75(19)
O2	C2	C3	124.03(18)
C4	C5	C6	120.72(19)
C7	C6	C5	119.64(19)
C12	C11	C3	117.25(16)
C12	C11	C10	109.84(17)
C10	C11	C3	60.66(13)
C14	C13	C12	117.8(2)
C8	C7	C6	120.09(19)
C8	C9	C4	120.19(19)
C12	C17	S1	113.28(16)

Atom	Atom	Atom	Angle/°
C16	C17	S1	125.47(18)
C16	C17	C12	121.2(2)
C3	C10	S1	119.90(14)
C11	C10	S1	110.98(15)
C11	C10	C3	61.10(13)
C7	C8	C9	120.2(2)
C16	C15	C14	121.1(2)
C13	C14	C15	121.0(2)
C15	C16	C17	118.8(2)

The X ray crystal structures of compounds **3aa** and **3ba** have been previously reported (CCDC numbers: 1576359 and 1576357, respectively).[8]

7 References

1   I.D. Jurberg and H. M. L. Davies, *Chem. Sci.*, 2018, **9**, 5112-5118.

2   a) G. Özüduru, T. Schubach and M. M. K. Boysen, *Org. Lett.*, 2012, **14**, 4990-4993; b) L. Grehn and U. Ragnarsson, *Angew. Chem. Int. Ed.*, 1984, **23**, 296-301.

3   J. Fu, N. Wurzer, V. Lehner, O. Reiser, H. M. L. Davies, *Org. Lett.*, 2019, **21**, 6102-6106

4   J. E. Jakobsson, G. Gronnevik, P. J. Riss, *Chem. Commun.*, 2017, **53**, 12906-12909

5   T. Jaschinski and M. Hiersemann, *Org. Lett.*, 2012, **14**, 4114-4117.

6   H. M. L Davies, T. Hansen and M. R. Churchill, *J. Am. Chem. Soc.*, 2000, **122**, 3063-3070.

7   W.-W. Chan, S.-H. Yeung, Z. Zhou, A. S. C. Chan. and W.-Y. Yu, *Org. Lett.*, 2010, **12**, 604-607.

8   V. Lehner, H. M. L. Davies and O. Reiser, *Org. Lett.*, 2017, **19**, 4722-4725.

9   S. Budde, F. Goerdeler, J. Floß, P. Kreitmeier, E. F. Hicks, O. Moscovitz, P. H. Seeberger, H. M. L. Davies and O. Reiser, *Org. Chem. Front.*, 2020, **7**, 1789-1795.

10   S. Gratia, K. Mosesohn and S. T. Diver, *Org. Lett.*, 2016, **18**, 5320-5323

11   S. Jana, F. Li, C. Empel, D. Verspeek, P. Aseeva and R. M. Koenigs, *Chem. Eur. J.*, 2020, **26**, 2586-2591.

12   SCALE3ABS, CrysAlisPro, Aglient Technologies Inc. Oxford and GB, 2015; (b) G.M. Sheldrick, SADABS, Bruker AXS, Madison and USA, 2007.

13   (a) R. C. Clark, J. S. Reid, *Acta Cryst. A*, 1995, **51,** 887-897; (b) CrysAlisPro, version 171.39.37b, Agilent Technologies Inc., Oxford and GB, 2017.

14   G. M. Sheldrick, *Acta Cryst. A*, 2015, **71**, 3-8.

15   O. V. Dolomanov, L. J. Bourhis, R. J. Gildea, J. A. K. Howard, H. Puschmann, *J. Appl. Crystallogr*. 2009, **42**, 339-341.

16   G. M. Sheldrick, *Acta Cryst. A*, 2008, **64**, 112-22.